

Dependent Random Partitions by Shrinking Toward an Anchor

David B. Dahl^{*†}

Department of Statistics, Brigham Young University

Richard L. Warr[‡]

Department of Statistics, Brigham Young University

Thomas P. Jensen[§]

Berry Consultants LLC

October 28, 2024

Abstract

Although exchangeable processes from Bayesian nonparametrics have been used as a generating mechanism for random partition models, we deviate from this paradigm to explicitly incorporate clustering information in the formulation of our random partition model. Our shrinkage partition distribution takes any partition distribution and shrinks its probability mass toward an anchor partition. We show how this provides a framework to model hierarchically-dependent and temporally-dependent random partitions. The shrinkage parameter controls the degree of dependence, accommodating at its extremes both independence and complete equality. Since *a priori* knowledge of items may vary, our formulation allows the degree of shrinkage toward the anchor to be item-specific. Our random partition model has a tractable normalizing constant which allows for standard Markov chain Monte Carlo algorithms for posterior sampling. We prove intuitive theoretical properties for our distribution and compare it to related partition distributions. We show that our model provides better out-of-sample fit in a real data application.

Keywords: Bayesian nonparametrics; Chinese restaurant process; Hierarchically dependent partitions; Temporally dependent partitions; Spatiotemporal random partitions.

*The authors thank the editor, associate editor, and two reviewers for their time and constructive comments which significantly improved the manuscript. The authors report no conflicts of interest.

[†]ORCID: 0000-0002-8173-1547

[‡]ORCID: 0000-0001-8508-3105

[§]ORCID: 0009-0000-0015-3881

1 Introduction

Random partition models are flexible Bayesian prior distributions which accommodate heterogeneity and the borrowing of strength by postulating that data or parameters are generated from latent clusters. Exchangeable random partition models arise from Bayesian nonparametric (BNP) models, which are very flexible and often involve rich modeling techniques applied to specific problems. In the presence of additional information that ought to influence the partition, the exchangeability constraint is untenable and researchers have developed nonexchangeable random partition models that are *not* obtained by marginalizing over a random measure G . Examples include Müller et al. (2011), Blei and Frazier (2011), Airoldi et al. (2014), and Dahl et al. (2017) which use covariates or distances to influence a partition distribution. Some have sought partition distributions which directly incorporate prior knowledge on the partition itself. Rather than incorporating covariates or distances in a partition distribution, one might wish to use a “best guess” as to the value of the partition, yet may not be completely certain and therefore may be unwilling to fix the partition on this value. Instead, a modeler may wish to use a partition distribution that is anchored on this “best guess” partition yet allow for deviations from it.

We introduce a partition distribution with a *shrinkage* parameter ω that governs the concentration of probability mass between two competing elements: a *baseline* partition distribution p_b and an *anchor* partition μ . We call our distribution the shrinkage partition (SP) distribution. Our approach builds on the pioneering work of Smith and Allenby (2020)’s location scale partition (LSP) and Paganin et al. (2021)’s centered partition process (CPP). Our SP distribution and both the LSP and CPP distributions are influenced by an anchor partition (called the “location” partition and the “centered” partition in their respective papers). However, the LSP depends on the arbitrary ordering of the data and the distribution of deviations from the anchor partition is immutable and intrinsically embedded, which limits modeling flexibility. Both our SP distribution and the CPP allow for any baseline partition

distribution, but the probability mass function (pmf) of the CPP is only specified up to the normalizing constant. The nature of the combinatorics makes the normalizing constant intractable, so the shrinkage parameter must be fixed using a computationally intensive cross-validation procedure and posterior inference on hyperparameters (e.g., the shrinkage parameter) is not practically feasible.

In contrast, our SP distribution has several desirable properties. First, the SP has a tractable normalizing constant, so standard Markov chain Monte Carlo (MCMC) techniques can be used for posterior inference on hyperparameters. Second, the SP does not depend on the order in which data are observed, making the data analysis invariant to what may be an arbitrary ordering. Third, the SP allows for any baseline partition distribution to govern the distribution of partitions informed by the anchor partition. Fourth, prior knowledge about the clustering of items may be different across the items and our SP is unique in allowing differential shrinkage toward the anchor.

Further, whereas the LSP and CPP were introduced as prior distributions for a single partition in situations where the modeler has a prior guess as to the value of the partition, we note that our formulation — in addition to being suitable for this case — also permits building models for dependent random partitions. [Page et al. \(2022\)](#) was the first to directly model temporally-dependent partitions that are evenly spaced in time. Our approach adds flexibility, permitting temporally-dependent random partition models that are not necessarily observed on a uniformly-spaced grid. Further, our SP permits not only temporal dependence, but other forms of dependence. [Camerlenghi et al. \(2019\)](#) and [Argiento et al. \(2020\)](#) show how to build hierarchical clustering models, however, as demonstrated in [Page et al. \(2022\)](#) dependence induced between partitions via random measures is somewhat limited. [Page et al. \(2022\)](#) showed that to achieve the full spectrum of dependence, from independence to equality, dependence must be induced directly on the partitions. We believe that our SP is the first to allow hierarchically-dependent partitions induced directly on the

partitions. [Song et al. \(2023\)](#) recently used our SP distribution as a basis for their innovative hierarchical bi-clustering model of mouse-tracking data. In contemporaneous work, [Paganin et al. \(2023\)](#) and [Dombowsky and Dunson \(2023\)](#) are two recent pre-prints on dependent random partitions.

The SP distribution scales well in the number of items being clustered. It has properties that one would expect in a partition distribution, such as the ability to control the distribution of the number of subsets, influence the distribution of cluster sizes, and generally behaves like other partition distributions in the literature, with the added feature of shrinking toward an anchor partition. Software implementing our SP distribution is available as an R package based on Rust (<https://github.com/dbdahl/gourd-package>).

The remainder of the paper is organized as follows. In [Section 2](#), we review the LSP and CPP and put them in common notation for ease in understanding the novelty of our SP distribution, which is detailed in [Section 3](#). Properties of the SP distribution are detailed in [Section 4](#) and models for dependent partition models based on the SP distribution are discussed in [Section 5](#). An empirical study in [Section 6](#) shows that our SP distribution, based on 10-fold cross validation, compares favorably to the LSP and CPP for a single partition and that our SP can be used for hierarchically-dependent and temporally-dependent partitions to improve performance beyond what is possible with models that ignore dependence among partitions.

2 Existing Distributions Indexed by a Partition

Our shrinkage partition distribution itself was inspired by [Paganin et al. \(2021\)](#)’s CPP and [Smith and Allenby \(2020\)](#)’s LSP. A key parameter in all three distributions is what we term the anchor partition $\boldsymbol{\mu}$, a partition of the integers $\{1, \dots, n\}$ which represents the *a priori* estimate of the population partition. The anchor partition plays the same role as the “centered” partition in the CPP and the “location” partition in the LSP. As noted by

Dahl et al. (2021), words like “centered” or “location” may be misnomers. We use the term “anchor” to suggest that the probability distribution is “tethered to” — but not “centered on” or “located at” — the anchor partition $\boldsymbol{\mu}$. How closely the partition distribution reflects $\boldsymbol{\mu}$ is a function of what we term the shrinkage parameter ω .

In this paper the anchor partition $\boldsymbol{\mu}$ is expressed in terms of cluster labels $\boldsymbol{\mu} = (\mu_1, \dots, \mu_n)$ such that two items have the same label (i.e., $\mu_i = \mu_j$) if and only if they belong to the same subset in the anchor partition. Likewise, we use $\boldsymbol{\pi}$ to denote the vector of cluster labels of a random partition. Cluster labels are assumed to be in canonical form, i.e., cluster label “1” is used for the first item (and all items clustered with it), cluster label “2” is used for the next item (and all items clustered with it) that is not clustered with the first item, etc. Studying the pmf of each distribution helps one see the similarities with our SP distribution, and what motivated us to develop our new partition distribution. For the sake of comparison, we express each distribution in common notation.

2.1 Centered Partition Process

The CPP of Paganin et al. (2021) is formed from a baseline partition distribution $p_b(\boldsymbol{\pi})$ and a distance function $d(\boldsymbol{\pi}, \boldsymbol{\mu})$ which measures the discrepancy between two partitions. The pmf of the CPP is $p_{\text{cp}}(\boldsymbol{\pi} \mid \boldsymbol{\mu}, \omega, d, p_b) \propto p_b(\boldsymbol{\pi}) \exp(-\omega d(\boldsymbol{\pi}, \boldsymbol{\mu}))$, where $\omega \geq 0$ is a univariate shrinkage parameter controlling the magnitude of the penalty for discrepancy with the anchor partition $\boldsymbol{\mu}$. The baseline partition distribution $p_b(\boldsymbol{\pi})$ will likely depend on other parameters (e.g., a concentration parameter) but we suppress them here for simplicity. Note that $p_{\text{cp}}(\boldsymbol{\pi} \mid \boldsymbol{\mu}, \omega, d, p_b)$ reduces to the baseline partition distribution $p_b(\boldsymbol{\pi})$ as $\omega \rightarrow 0$. Conversely, as $\omega \rightarrow \infty$, all probability concentrates on the anchor partition $\boldsymbol{\mu}$, i.e. $p_{\text{cp}}(\boldsymbol{\pi} = \boldsymbol{\mu} \mid \boldsymbol{\mu}, \omega, d, p_b) \rightarrow 1$. While any distance function $d(\boldsymbol{\pi}, \boldsymbol{\mu})$ for partitions could be used, Paganin et al. (2021) focus on the variation of information (Meilă, 2007; Wade and Ghahramani, 2018). We use the notation $\boldsymbol{\pi} \sim \text{CPP}(\boldsymbol{\mu}, \omega, d, p_b)$ for a partition whose

distribution is the CPP with anchor partition $\boldsymbol{\mu}$, shrinkage parameter ω , distance function d , and baseline distribution p_b .

A key challenge with the CPP is that the pmf is only specified up to proportionality. While the normalizing constant can theoretically be obtained through enumeration, the number of possible partitions of n items (as given by the Bell number) quickly makes enumeration infeasible beyond 20 or so items. The lack of a normalizing constant precludes posterior inference on other parameters associated with the baseline distribution (e.g., a concentration parameter). Further, as a practical matter, the shrinkage parameter ω must be fixed for data analysis, making the CPP unsuitable for modeling dependent partitions.

2.2 Location-Scale Partition Distribution

As the name implies, [Smith and Allenby \(2020\)](#) originally expressed their location-scale partition (LSP) distribution using a scale parameter. We reparameterize the LSP’s pmf, for the sake of comparison, to use a univariate shrinkage parameter ω , which is the reciprocal of their original scale parameter. The LSP has a constructive definition, in which a partition $\boldsymbol{\pi}$ is obtained by sequentially allocating items. There may be common values among π_1, \dots, π_i and we let $\{\pi_1, \dots, \pi_i\}$ denote the set of unique cluster labels after the i^{th} item is allocated and, therefore, $|\{\pi_1, \dots, \pi_i\}|$ is the cardinality of that set or, in other words, the number of clusters in the partition after item i is allocated. Note that, for the LSP, the order in which items are allocated affects the probability of a partition, making data analysis subject to what is often an arbitrary ordering. To overcome this deficiency and to make the comparisons in [Section 6](#) more fair, we generalize the original LSP using a technique of [Dahl et al. \(2017\)](#). Specifically, items are allocated in an order given by a permutation $\boldsymbol{\sigma} = (\sigma_1, \dots, \sigma_n)$ of the integers $\{1, \dots, n\}$, where the k^{th} item allocated is the σ_k^{th} item in the model or dataset, and a uniform prior is placed on the permutation $\boldsymbol{\sigma}$. Thus the LSP’s modified pmf is:

$$p_{\text{lsp}}(\boldsymbol{\pi} \mid \boldsymbol{\mu}, \omega, \boldsymbol{\sigma}) = \prod_{k=1}^n \text{Pr}_{\text{lsp}}(\pi_{\sigma_k} = c \mid \pi_{\sigma_1}, \dots, \pi_{\sigma_{k-1}}, \boldsymbol{\mu}, \omega, \boldsymbol{\sigma}),$$

where by definition $\Pr_{\text{lsp}}(\pi_{\sigma_1} = 1 \mid \boldsymbol{\mu}, \omega, \boldsymbol{\sigma}) = 1$ and for $k = 2, \dots, n$:

$$\Pr_{\text{lsp}}(\pi_{\sigma_k} = c \mid \pi_{\sigma_1}, \dots, \pi_{\sigma_{k-1}}, \boldsymbol{\mu}, \omega, \boldsymbol{\sigma}) \propto \quad (1)$$

$$\begin{cases} \frac{1 + \omega \sum_{j=1}^{k-1} \mathbb{I}\{\pi_{\sigma_j} = c\} \mathbb{I}\{\mu_{\sigma_j} = \mu_{\sigma_k}\}}{1 + |\{\mu_{\sigma_1}, \dots, \mu_{\sigma_{k-1}}\}| + \omega \sum_{j=1}^{k-1} \mathbb{I}\{\pi_{\sigma_j} = c\}} & \text{for } c \in \{\pi_{\sigma_1}, \dots, \pi_{\sigma_{k-1}}\} \\ \frac{1 + \omega \mathbb{I}\left\{\sum_{j=1}^{k-1} \mathbb{I}\{\mu_{\sigma_j} = \mu_{\sigma_k}\} = 0\right\}}{1 + |\{\mu_{\sigma_1}, \dots, \mu_{\sigma_{k-1}}\}| + \omega} & \text{for } c = |\{\pi_{\sigma_1}, \dots, \pi_{\sigma_{k-1}}\}| + 1. \end{cases}$$

Following [Dahl et al. \(2017\)](#), the key to obtaining a normalizing constant for the LSP and our SP distribution comes from sequential allocation.

We use the notation $\boldsymbol{\pi} \sim \text{LSP}(\boldsymbol{\mu}, \omega)$ for a partition whose distribution is our modification of the LSP, marginalizing over $\boldsymbol{\sigma}$. We note that using a permutation parameter $\boldsymbol{\sigma}$ (as introduced by [Dahl et al. 2017](#)) and marginalizing over it makes the LSP invariant to the ordering of the data. However, this invariance to the ordering of the data does not imply the revised LSP (nor our SP distribution) is exchangeable since the probability of a partition under those distributions is not solely a function of cluster sizes. See [Ghosal and van der Vaart \(2017, pg. 438\)](#) for the definition of exchangeable random partitions. As with the CPP, $p_{\text{lsp}}(\boldsymbol{\pi} = \boldsymbol{\mu} \mid \boldsymbol{\mu}, \omega) \rightarrow 1$ as $\omega \rightarrow \infty$.

Noticeably absent from the LSP are parameters to control the distribution beyond the anchor partition $\boldsymbol{\mu}$ and the shrinkage ω . As $\omega \rightarrow 0$, the sequential allocation probabilities found in [\(1\)](#) reduce to a uniform selection among existing clusters and a new cluster. There is no mechanism to control the number of clusters. The LSP's baseline partition distribution is "hardwired" into its pmf and is obtained when $p_{\text{lsp}}(\boldsymbol{\pi} \mid \boldsymbol{\mu}, \omega = 0)$. Note that this partition distribution is a special case of [Jensen and Liu \(2008\)](#)'s distribution with mass parameter fixed at 1.

3 Shrinkage Partition Distribution

3.1 Probability Mass Function

We now present the pmf of our SP distribution, which incorporates key strengths of both the CPP and the LSP, addresses some of their limitations, and adds modeling flexibility. Like the CPP and the LSP, the SP distribution uses an anchor partition $\boldsymbol{\mu}$. Both the CPP and the LSP have a single, real-valued shrinkage parameter $\omega \geq 0$, with larger shrinkage values producing higher concentrations of probability mass for partitions that are close to $\boldsymbol{\mu}$. In contrast, the SP distribution uses a vector-valued shrinkage $\boldsymbol{\omega} = (\omega_1, \dots, \omega_n)$ to permit item-specific knowledge and flexibility in how close realizations from the SP distribution are to the anchor partition $\boldsymbol{\mu}$. That is, $\omega_i \geq 0$ is idiosyncratic to the i^{th} item, although a modeler could simplify $\boldsymbol{\omega}$'s structure by making each entry equal or choose to have items in the particular subset of $\boldsymbol{\mu}$ all share the same shrinkage value (i.e., $\omega_i = \omega_j$ if $\mu_i = \mu_j$).

Like many other partition distributions, including the LSP, we adopted a sequential allocation construction for the SP distribution, with an important caveat. As it was originally defined, the LSP distribution implicitly uses a fixed permutation $\boldsymbol{\sigma} = (1, \dots, n)$, which makes the data analysis dependent on the ordering of the data. In some contexts (e.g., time series), the item order may be meaningful. But most commonly, the permutation $\boldsymbol{\sigma}$ would be viewed as a nuisance parameter. Lacking prior knowledge for $\boldsymbol{\sigma}$, we recommend using the uniform distribution on $\boldsymbol{\sigma}$, that is, $p(\boldsymbol{\sigma}) = \frac{1}{n!}$. Marginalizing over $\boldsymbol{\sigma}$ has the effect of making the data analysis invariant to the order of the data. We also place a practical constraint on the baseline partition distribution p_b : it must have an explicit allocation rule Pr_b that conditions on previously allocated items. Thus $p_b(\boldsymbol{\pi}) = \prod_{k=1}^n \text{Pr}_b(\pi_{\sigma_k} \mid \pi_{\sigma_1}, \dots, \pi_{\sigma_{k-1}}) = \prod_{k=1}^n \text{Pr}_b(\pi_{\sigma_k} \mid \boldsymbol{\pi}_{\sigma_{1:k-1}})$, where $\boldsymbol{\pi}_{\sigma_{1:k-1}} = \pi_{\sigma_1}, \dots, \pi_{\sigma_{k-1}}$. The function Pr_b may well have other parameters (e.g., a concentration parameter) but we suppress these here for generality and simplicity. The function p_b may be an exchangeable partition probability function

(EPPF) from, for example, the Ewens distribution (Ewens, 1972; Pitman, 1995), but we are not limited to exchangeable priors and only require a sequential allocation rule. We call this sequential allocation rule Pr_b a conditional allocation probability function (CAPF).

The CPP utilizes a distance function between $\boldsymbol{\pi}$ and $\boldsymbol{\mu}$ such as the Binder loss (Binder, 1978) or the variation of information (Meilă, 2007; Wade and Ghahramani, 2018). Analogously, the SP’s anchor partition distribution uses a function inspired by the general form of Binder loss (Dahl et al., 2022). This function, denoted Pr_a , rewards allocations which agree with $\boldsymbol{\mu}$ while simultaneously penalizing or rewarding larger clusters through a real-valued grit parameter ψ . The function is presented in CAPF form:

$$\text{Pr}_a(\pi_{\sigma_k} = c \mid \boldsymbol{\pi}_{\sigma_{1:k-1}}, \boldsymbol{\mu}, \boldsymbol{\omega}, \boldsymbol{\sigma}, \psi) \propto \exp\left(\frac{\omega_{\sigma_k}}{k-1} \sum_{j=1}^{k-1} \omega_{\sigma_j} \mathbb{I}\{\pi_{\sigma_j} = c\} (\mathbb{I}\{\mu_{\sigma_j} = \mu_{\sigma_k}\} - \psi)\right) \quad (2)$$

for $c \in \{\pi_{\sigma_1}, \dots, \pi_{\sigma_{k-1}}, |\{\pi_{\sigma_1}, \dots, \pi_{\sigma_{k-1}}\}| + 1\}$. Notationally, $|\{\pi_{\sigma_1}, \dots, \pi_{\sigma_{k-1}}\}|$ is the number of clusters before allocating the σ_k^{th} item. The pmf of the SP distribution is:

$$p_{\text{SP}}(\boldsymbol{\pi} \mid \boldsymbol{\mu}, \boldsymbol{\omega}, \boldsymbol{\sigma}, \psi, p_b) = \prod_{k=2}^n \text{Pr}_{\text{SP}}(\pi_{\sigma_k} \mid \boldsymbol{\pi}_{\sigma_{1:k-1}}, \boldsymbol{\mu}, \boldsymbol{\omega}, \boldsymbol{\sigma}, \psi, p_b), \quad (3)$$

where

$$\text{Pr}_{\text{SP}}(\pi_{\sigma_k} \mid \boldsymbol{\pi}_{\sigma_{1:k-1}}, \boldsymbol{\mu}, \boldsymbol{\omega}, \boldsymbol{\sigma}, \psi, p_b) \propto \text{Pr}_b(\pi_{\sigma_k} \mid \boldsymbol{\pi}_{\sigma_{1:k-1}}) \times \text{Pr}_a(\pi_{\sigma_k} \mid \boldsymbol{\pi}_{\sigma_{1:k-1}}, \boldsymbol{\mu}, \boldsymbol{\omega}, \boldsymbol{\sigma}, \psi). \quad (4)$$

We note that, to simplify notation, we are conditioning on $\boldsymbol{\mu}$, $\boldsymbol{\omega}$, and $\boldsymbol{\sigma}$, however, the probabilities defined in (2) – (4) are conditionally dependent on only some elements of these vectors. For a random partition $\boldsymbol{\pi}$, we use the notation $\boldsymbol{\pi} \sim \text{SP}(\boldsymbol{\mu}, \boldsymbol{\omega}, \boldsymbol{\sigma}, \psi, p_b)$ to denote the partition has a SP distribution with an anchor partition $\boldsymbol{\mu}$, a shrinkage vector $\boldsymbol{\omega}$, a permutation $\boldsymbol{\sigma}$, and a baseline distribution p_b . When marginalizing over the permutation parameter with a uniform prior (thereby making the distribution invariant to the ordering of the data), we use the notation $\boldsymbol{\pi} \sim \text{SP}(\boldsymbol{\mu}, \boldsymbol{\omega}, \psi, p_b)$. Similar to the revised LSP introduced in Section 2.2, we note that invariance to the ordering of the data does not imply that the SP is exchangeable.

From (3), it is clear that the allocation of items to subsets in a partition are sequential. However, the SP distribution is similar in form to the CPP in that the allocation of each item depends on the baseline partition distribution p_b and its compatibility with the anchor partition $\boldsymbol{\mu}$. The CPP, however, applies this trade-off globally, whereas our SP distribution does so on a sequential, item-by-item basis. At the k^{th} step, note that there are only $|\{\pi_{\sigma_1}, \dots, \pi_{\sigma_{k-1}}\}| + 1$ possible allocations for σ_k . Thus, the normalizing constant needed for (4) is readily computed for any n , which easily permits posterior inference on any of the parameters in the SP distribution using standard MCMC techniques.

Recall that the CPP allows for different distance functions and the chosen loss function implicitly favors some partitions over others. For example, the Binder loss tends to produce many small clusters whereas VI tends to produce fewer clusters (Rastelli and Friel, 2018; Dahl et al., 2022). Our grit parameter ψ in (2) provides a similar mechanism to control the propensity for small clusters. A key difference, however, is that our grit parameter ψ is continuous and a prior can be placed on it, whereas the CPP’s distance function must be chosen and fixed.

3.2 Baseline Distributions

The baseline distribution p_b is a key component of both the CPP and SP, which affords flexibility to the modeler. Here we discuss a few obvious choices for p_b and emphasize that others may be desired for any given situation. Conditional allocation probability functions are one way to characterize probability mass functions for partition distributions and are used in the SP distribution. CAPFs rely on items being sequentially allocated to clusters in the partition. Although most partition distributions can be viewed as sequentially allocated processes, those that cannot may not have tractable CAPFs. In this section, we examine a few partition distributions that could serve as a baseline distribution for the SP distribution and provide their associated CAPFs.

The two most common partition distributions are the Ewens (Ewens, 1972; Pitman, 1995) and the Ewens-Pitman (Pitman and Yor, 1997) distributions (also referred to as the one-parameter and two-parameter Chinese restaurant process, respectively). The CAPF for the Ewens-Pitman partition distribution is:

$$\Pr_b(\pi_{\sigma_k} = c \mid \boldsymbol{\pi}_{\sigma_{1:k-1}}, \alpha, \delta, \boldsymbol{\sigma}) = \begin{cases} \frac{(\sum_{j=1}^{k-1} I(\pi_{\sigma_j} = c)) - \delta}{k-1+\alpha} & \text{for } c \in \{\pi_{\sigma_1}, \dots, \pi_{\sigma_{k-1}}\} \\ \frac{\alpha + \delta |\{\pi_{\sigma_1}, \dots, \pi_{\sigma_{k-1}}\}|}{k-1+\alpha} & \text{for } c = |\{\pi_{\sigma_1}, \dots, \pi_{\sigma_{k-1}}\}| + 1 \end{cases} \quad (5)$$

Although this distribution is invariant to item allocation order, we include a permutation parameter in the CAPF for notational consistency. The CAPF of the Ewens distribution can be obtained by setting $\delta = 0$ in (5). Both the Ewens and Ewens-Pitman distributions have the “rich-get-richer” property which can be adjusted to some extent in the Ewens-Pitman distribution through the discount parameter δ . We use $\text{CRP}(\alpha)$ to denote the Ewens-Pitman distribution with concentration α and discount $\delta = 0$.

The uniform partition (UP) distribution is exchangeable and is a very simple partition distribution. To be used as a baseline distribution for the SP distribution, its CAPF is needed. To our knowledge, the sequential allocation rule for the uniform partition distribution is not contained in the literature elsewhere and we provide it here. First, the total number of items to be partitioned, denoted n , must be fixed and known. Then, at the σ_k^{th} item’s allocation, one must know the number of subsets allocated thus far in the partition (i.e., $|\{\pi_{\sigma_1}, \dots, \pi_{\sigma_{k-1}}\}|$) and also the number of items left to allocate (i.e., $n - k + 1$). Now consider an extension of the Bell number $B(a, b)$, defined recursively by the following formulas: $B(0, b) = 1$ and $B(a + 1, b) = bB(a, b) + B(a, b + 1)$, for all $a, b \in \mathbb{N}$ (the nonnegative integers). We note that $B(a) \equiv B(a, 0)$ is the a^{th} Bell number; additional information about the extension of the Bell number is included in Appendix A. The CAPF for the UP

distribution is:

$$\Pr_b(\pi_{\sigma_k} = c \mid \boldsymbol{\pi}_{\sigma_{1:k-1}}, n, \boldsymbol{\sigma}) = \begin{cases} \frac{B(n-k, |\{\pi_{\sigma_1}, \dots, \pi_{\sigma_{k-1}}\}|)}{B(n-k+1, |\{\pi_{\sigma_1}, \dots, \pi_{\sigma_{k-1}}\}|)} & \text{for } c \in \{\pi_{\sigma_1}, \dots, \pi_{\sigma_{k-1}}\} \\ \frac{B(n-k, |\{\pi_{\sigma_1}, \dots, \pi_{\sigma_{k-1}}\}|+1)}{B(n-k+1, |\{\pi_{\sigma_1}, \dots, \pi_{\sigma_{k-1}}\}|)} & \text{for } c = |\{\pi_{\sigma_1}, \dots, \pi_{\sigma_{k-1}}\}| + 1, \end{cases} \quad (6)$$

for $k \in \{2, \dots, n\}$. When $k = 1$, the CAPF for the UP distribution simply equals 1.

The Jensen-Liu partition (JLP) distribution was introduced by [Jensen and Liu \(2008\)](#) and later named in [Casella et al. \(2014\)](#). It places a uniform probability of allocating to any existing cluster and a distinct probability of forming a new cluster. Unlike the previously mentioned distributions in this section, the JLP is not exchangeable. The CAPF for the JLP (endowed with a permutation parameter) is:

$$\Pr_b(\pi_{\sigma_i} = c \mid \boldsymbol{\pi}_{\sigma_{1:i-1}}, \alpha, \boldsymbol{\sigma}) = \begin{cases} \frac{1}{|\{\pi_{\sigma_1}, \dots, \pi_{\sigma_{i-1}}\}| + \alpha} & \text{for } c \in \{\pi_{\sigma_1}, \dots, \pi_{\sigma_{i-1}}\} \\ \frac{\alpha}{|\{\pi_{\sigma_1}, \dots, \pi_{\sigma_{i-1}}\}| + \alpha} & \text{for } c = |\{\pi_{\sigma_1}, \dots, \pi_{\sigma_{i-1}}\}| + 1. \end{cases} \quad (7)$$

There are other possible baseline partition distributions. [Dahl et al. \(2017\)](#) introduces the Ewens-Pitman attraction (EPA) distribution, which generalizes the Ewens-Pitman distribution when pairwise distances (or similarities) between items are known. Using the EPA distribution would allow one to incorporate covariates into the partitioning of items by converting the covariates to similarities between items. Another recent addition to partition distributions is the Allelic partition distribution ([Betancourt et al., 2022](#)). This distribution was developed specifically to have the microclustering property (that is, partitions contain many clusters in which there are relatively few items in each). This partition behavior is in stark contrast to the Ewens distribution, which favors large cluster sizes. Product partition models (PPMs [Hartigan, 1990](#)) can be used as a baseline in the SP distribution. Suitable extensions of PPMs incorporate covariates ([Müller et al., 2011](#); [Park and Dunson, 2010](#)) or those that add spatial structure with covariates ([Page and Quintana, 2016](#)).

4 Effect of Shrinkage and Grit Parameters

An intuitive way to think about the shrinkage partition (SP) distribution is to view it as a compromise between a baseline partition distribution p_b and the anchor partition $\boldsymbol{\mu}$. This compromise is controlled by the shrinkage parameter $\boldsymbol{\omega}$ and the grit parameter ψ . In this section, we investigate in more detail how these parameters influence the SP distribution. Proofs of the theorems are found in Appendix B.

4.1 Extremes and Smooth Evolution Between Extremes

The degree of compromise between the baseline partition distribution p_b and the anchor partition $\boldsymbol{\mu}$ is governed by the shrinkage parameter $\boldsymbol{\omega} = (\omega_1, \dots, \omega_n)$. In one extreme case, where each idiosyncratic shrinkage ω_i is relatively large, the SP distribution assigns probability mass to partitions that are very similar to the anchor partition $\boldsymbol{\mu}$ and, in the limit, the distribution becomes a point mass distribution at the anchor partition $\boldsymbol{\mu}$. In the other extreme case, i.e., when the idiosyncratic shrinkages ω_i all equal zero, the SP reduces to the baseline distribution p_b and the anchor partition $\boldsymbol{\mu}$ has no influence in the SP's pmf. We formally present these properties below.

Theorem 1. *Let $\boldsymbol{\rho}_1$ be the partition with all n items assigned to a single cluster, $\boldsymbol{\rho}_n$ be the partition with n items each assigned to a unique cluster, $\boldsymbol{\pi} \sim SP(\boldsymbol{\mu}, \boldsymbol{\omega}, \psi, p_b)$ with $p_b(\boldsymbol{\mu}) > 0$, and $\boldsymbol{\omega} = \omega \times (1, \dots, 1)$:*

- a) if $\omega = 0$, then $\boldsymbol{\pi} \sim p_b$. *[Diffusion to the baseline dist'n]*
- b) if $\psi \in (0, 1)$ then $\lim_{\omega \rightarrow \infty} Pr(\boldsymbol{\pi} = \boldsymbol{\mu}) = 1$ *[Anchor partition consistency]*
- c) if $\psi \in (-\infty, 0)$ then $\lim_{\omega \rightarrow \infty} Pr(\boldsymbol{\pi} = \boldsymbol{\rho}_1) = 1$
- d) if $\psi \in (1, \infty)$ then $\lim_{\omega \rightarrow \infty} Pr(\boldsymbol{\pi} = \boldsymbol{\rho}_n) = 1$.

Recall that $\boldsymbol{\pi}$ and $\boldsymbol{\mu}$ are vectors of cluster labels. When statements such as $\boldsymbol{\pi} = \boldsymbol{\mu}$ are made,

we imply that they are in the same equivalence class, that is, their cluster labels encode the same partition.

Note that as the shrinkage ω goes to infinity, the desirable behavior that $\Pr(\boldsymbol{\pi} = \boldsymbol{\mu}) = 1$ only occurs when $\psi \in (0, 1)$. Of course, for finite ω , there could be situations in which better model fit is obtained by relaxing the restriction that $\psi \in (0, 1)$. We feel, however, that it would be better in such situations to revisit the choice for the baseline distribution p_b to influence the number and size of clusters. As such, we recommend restricting ψ to the unit interval and do so throughout the rest of the paper.

Between the extreme cases for the shrinkage ω (i.e., zero and infinity) and under certain conditions, the probability of the anchor partition is monotonically increasing in ω .

Theorem 2. *For any $\delta > 0$ and p_b such that $0 < p_b(\boldsymbol{\mu}) < 1$, if $\boldsymbol{\pi}_1 \sim SP(\boldsymbol{\mu}, \boldsymbol{\omega}, \psi, p_b)$ and $\boldsymbol{\pi}_2 \sim SP(\boldsymbol{\mu}, \boldsymbol{\omega} + \delta, \psi, p_b)$ with $\boldsymbol{\omega} = \omega \times (1, \dots, 1)$, $0 \leq \omega < \infty$ and $\psi \in (0, 1)$, then $\Pr(\boldsymbol{\pi}_1 = \boldsymbol{\mu}) < \Pr(\boldsymbol{\pi}_2 = \boldsymbol{\mu})$.*

This theorem implies that ω controls how “close” in probability the SP distribution is to the anchor partition $\boldsymbol{\mu}$. Additionally, this closeness to $\boldsymbol{\mu}$ is strictly increasing as ω increases.

Whereas Theorem 2 illustrates monotonically increasing probability for the anchor $\boldsymbol{\mu}$ as a function of increasing ω , in fact the entire distribution is getting closer to a point mass distribution at $\boldsymbol{\mu}$. In the following theorem we show the Kullback-Leibler (KL) divergence and the total variation (TV) distance between the SP distribution and a point mass distribution at the anchor decreases monotonically with increasing ω . We also show that the expectation of the Rand index (RI), a measure of agreement between partitions, converges to 1 as ω goes to infinity, implying the partitions are identical asymptotically.

Theorem 3. *Consider two partition distributions: i) $p_{\boldsymbol{\mu}}$, a point mass at the anchor partition $\boldsymbol{\mu}$, and ii) $SP(\boldsymbol{\mu}, \boldsymbol{\omega}, \psi, p_b)$ such that $\boldsymbol{\omega} = \omega \times (1, \dots, 1)$ with $0 \leq \omega < \infty$, $\psi \in (0, 1)$, and $0 < p_b(\boldsymbol{\mu}) < 1$. If $\boldsymbol{\mu} \sim p_{\boldsymbol{\mu}}$ and $\boldsymbol{\pi} \sim SP(\boldsymbol{\mu}, \boldsymbol{\omega}, \psi, p_b)$ then:*

- a) $D_{KL}(\boldsymbol{\mu}, \boldsymbol{\pi})$ is strictly decreasing as ω increases.

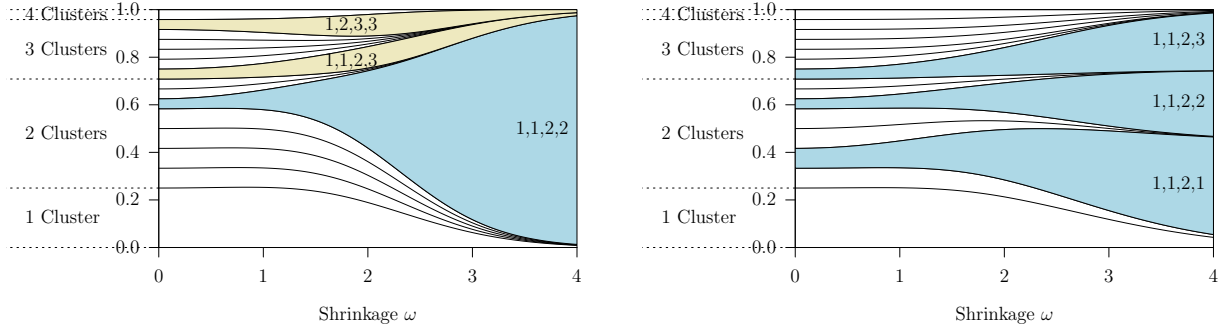


Figure 1: Left: The probabilities of all possible partitions for $n = 4$ items evolving as the shrinkage ω increases. As discussed in Section 4.1, the areas highlighted in blue show that the probability of the anchor partition begins to dominate as ω increases. Right: The evolution of SP's probabilities when $\omega_4 = 0$ and the others increase. As discussed in Section 4.2, the blue areas highlight the limiting partitions.

b) $D_{TV}(\boldsymbol{\mu}, \boldsymbol{\pi})$ is strictly decreasing as ω increases.

c) $E_{\boldsymbol{\mu}, \boldsymbol{\pi}} [RI(\boldsymbol{\mu}, \boldsymbol{\pi})] \rightarrow 1$ as $\omega \rightarrow \infty$.

Although not a true metric, the Kullback-Leibler divergence provides a sense of how relatively “close” two distributions are to each other. This theorem reinforces the concept that the SP distribution is a compromise between the baseline distribution p_b and the anchor partition $\boldsymbol{\mu}$. When $\omega = 0$, the SP distribution is identical to p_b , and $D(\boldsymbol{\mu}, \boldsymbol{\pi})$ is at its maximum. Then, as ω increases, $D(\boldsymbol{\mu}, \boldsymbol{\pi})$ strictly decreases, or in other words, the SP distribution moves away from p_b and toward the point mass distribution at $\boldsymbol{\mu}$.

Theorems 1, 2, and 3 provide intuition for the shrinkage parameter, which is reinforced with an illustrative example. Consider the SP distribution in which we marginalize over a uniform prior on the permutation $\boldsymbol{\sigma}$, we fix the grit ψ at 0.3, p_b is the CRP(1), and $\boldsymbol{\omega} = \omega \times (1, \dots, 1)$. The left plot in Figure 1 shows the evolution of the SP's probabilities of an anchor partition as a function of increasing ω . The plot shows the probabilities for the $B(4) = 15$ partitions of $n = 4$ items that are stacked so that, if a vertical line segment were drawn between 0 and 1 at some value of ω , then the line segment would be divided into 15

pieces, with the length of each piece representing the probability of one of the 15 partitions. The length of the vertical line segment in the blue region denotes the probability of the anchor partition $\boldsymbol{\mu} = (1, 1, 2, 2)$ which, when $\omega = 0$, is determined solely from the baseline distribution p_b and then converges to 1 as ω goes to infinity. The plot visually depicts an example of anchor partition consistency, diffusion to the baseline distribution, and the smooth evolution between these two extremes. Also note that the partitions $(1, 1, 2, 3)$ and $(1, 2, 3, 3)$ are shaded in yellow. These partitions are similar to the $\boldsymbol{\mu} = (1, 1, 2, 2)$ and therefore have increasing probability for small shrinkage ω which eventually gives way to the anchor $\boldsymbol{\mu} = (1, 1, 2, 2)$ for large ω . The upshot of these theorems and example is that the shrinkage parameter $\boldsymbol{\omega}$ smoothly controls the compromise between a baseline partition distribution p_b and the anchor partition $\boldsymbol{\mu}$. The SP distribution inherits clustering properties of p_b which are tempered by the anchor partition $\boldsymbol{\mu}$ based on the values of $\boldsymbol{\omega}$.

This compromise behavior is reminiscent of Müller et al. (2004) who showed how to define a novel distribution function as a convex linear combination of two distributions, e.g., $(1 - \epsilon)F + \epsilon F_0$, where $\epsilon \in [0, 1]$ controls the degree of compromise between F and F_0 . In our SP distribution, the compromise parameter is our vector-valued shrinkage parameter $\boldsymbol{\omega}$, and it induces a total variation distance that takes values in $[0, 1]$. As shown in the proof of Theorem 3, the total variation distance D_{TV} between the SP distribution and the point mass distribution at the anchor $\boldsymbol{\mu}$ equals one minus the probability of the anchor $\boldsymbol{\mu}$, i.e., in the left plot of Figure 1, one minus the length of a vertical line segment in blue for any given shrinkage ω . So, in this example with $n = 4$, D_{TV} is 0.96 when $\omega = 0$, decreases to 0.68 when $\omega = 2$, and equals 0.04 when $\omega = 4$. In a situation with n being much larger, the total variation distance is still easily computed for a fixed permutation and readily approximated through Monte Carlo methods for a random permutation.

4.2 Idiosyncratic Shrinkage Parameters

Recall that the SP distribution is parameterized with a vector-valued shrinkage parameter $\boldsymbol{\omega} = (\omega_1, \dots, \omega_n)$. Whereas the CPP and LSP have only a univariate shrinkage parameter ω to inform the compromise between the baseline distribution p_b and the anchor partition $\boldsymbol{\mu}$, our SP distribution allows for idiosyncratic shrinkages. The allowance of item-specific shrinkages $\omega_1, \dots, \omega_n$ offers unique flexibility in prior elicitation that is consequently not possible in existing distributions. Specifically, consider a data analysis scenario where there is strong prior knowledge regarding the clustering of a few items, but little or no prior knowledge regarding the clustering of the remaining items. In this case, the SP prior may avoid inadvertently imposing prior influence on less-understood relationships by setting corresponding shrinkage values to be relatively small or, at the extreme, 0 itself. Conversely, strong *a priori* clustering information about a few items can be expressed without fear of unduly affecting items which are not well understood.

For illustration, consider again an SP distribution in which $n = 4$, $\boldsymbol{\sigma}$ is integrated out of the model, $\psi = 0.3$, and p_b is CRP(1). Recall the scenario in Section 4.1 with the anchor $\boldsymbol{\mu} = (1, 1, 2, 2)$ and $\boldsymbol{\omega} = \omega \times (1, 1, 1, 1)$. Now assume instead there is no prior knowledge about the clustering of the fourth item (but we do have an indication that the first and second items are clustered together and are not clustered with the third item). That is, we are indifferent to $\boldsymbol{\mu} = (1, 1, 2, 1)$, $\boldsymbol{\mu} = (1, 1, 2, 2)$, and $\boldsymbol{\mu} = (1, 1, 2, 3)$, apart from beliefs about the number and size of clusters encoded within the baseline distribution p_b and the grit parameter ψ . In this case, we let $\boldsymbol{\omega} = \omega \times (1, 1, 1, 0)$ and any of these three values for the anchor $\boldsymbol{\mu}$ yield exactly the same partition distribution. The evolution of probabilities as ω increases is illustrated in the right plot of Figure 1. Notice that $(1, 1, 2, 1)$, $(1, 1, 2, 2)$, and $(1, 1, 2, 3)$ all retain probability as ω goes to infinity.

This example displays another key feature of the SP distribution when $\boldsymbol{\omega}$ contains both zero and non-zero values. We highlight that the SP distribution is invariant to the *a priori*

clustering of items with shrinkage parameter set to 0, i.e., $\omega_i = 0$. For example, since $\omega_4 = 0$, the probabilities for the SP distribution specified in the right pane of Figure 1 would remain unchanged if $\boldsymbol{\mu} = (1, 1, 2, 1)$ or $\boldsymbol{\mu} = (1, 1, 2, 3)$ instead of $\boldsymbol{\mu} = (1, 1, 2, 2)$.

Theorem 4. *If $\boldsymbol{\pi}_1 \sim SP(\boldsymbol{\mu}, \boldsymbol{\omega}, \boldsymbol{\sigma}, \psi, p_b)$ and $\boldsymbol{\pi}_2 \sim SP(\boldsymbol{\mu}^*, \boldsymbol{\omega}, \boldsymbol{\sigma}, \psi, p_b)$, where $\boldsymbol{\mu}$ and $\boldsymbol{\mu}^*$ are anchor partitions such that for every i and j where $\omega_i > 0$ and $\omega_j > 0$, $\mu_i = \mu_j$ if and only if $\mu_i^* = \mu_j^*$, then $\boldsymbol{\pi}_1$ and $\boldsymbol{\pi}_2$ are equal in distribution.*

The proof of Theorem 4 in Appendix B essentially says that an item with a shrinkage parameter of zero can be placed into any cluster in the anchor partition without affecting the probabilities of the SP distribution. This fits nicely with an intuitive Bayesian interpretation of having a shrinkage parameter set to zero and relieves the modeler from making an arbitrary choice that could affect the analysis. The behavior of the SP distribution is demonstrated in the right plot in Figure 1, and gives rise to what we refer to as “limiting partitions.” The definition of a limiting partition is:

Definition 1. *Let $\boldsymbol{\pi} \sim SP(\boldsymbol{\mu}, \boldsymbol{\omega}, \psi, p_b)$ with $\boldsymbol{\omega} = \omega \times (s_1, \dots, s_n)$ for scalars $s_i \in [0, \infty)$. A partition $\boldsymbol{\pi}$ which has non-zero probability as $\omega \rightarrow \infty$ is a limiting partition.*

When one or more idiosyncratic shrinkage parameters are set to zero and assuming $p_b(\boldsymbol{\mu}) > 0$, the SP distribution does not reduce to a point mass at $\boldsymbol{\mu}$ as ω becomes large. However, $\boldsymbol{\mu}$ remains a limiting partition and, if at least two items have $s_i > 0$, then the number of limiting partitions is less than the number that are possible under p_b . In the limit, this allows the SP distribution to force some items to be clustered and other items to be separated, and leave the remaining items to be randomly clustered according to p_b . The following theorem characterizes the limiting partitions.

Theorem 5. *Consider any baseline distribution p_b , anchor partition $\boldsymbol{\mu}$ and fixed partition $\boldsymbol{\rho}$, such that $p_b(\boldsymbol{\mu}) > 0$ and $p_b(\boldsymbol{\rho}) > 0$. For any $\boldsymbol{\omega} = \omega \times (s_1, \dots, s_n)$ with s_i either 0 or 1, and $\psi \in (0, 1)$, define \mathcal{Q} to be the set of index pairs (i, j) such that $\omega_i > 0$, $\omega_j > 0$, and $\mu_i = \mu_j$. If $\rho_i = \rho_j$ for all index pairs in \mathcal{Q} , then $\boldsymbol{\rho}$ is a limiting partition of $\boldsymbol{\pi} \sim SP(\boldsymbol{\mu}, \boldsymbol{\omega}, \psi, p_b)$.*

One interesting quantity of the SP distribution is the number of limiting partitions which exist. We know the number of possible partitions for n items with no constraints is the n^{th} Bell number, and on the other extreme, there is only one partition (a point mass) when all values in ω go to infinity. However, when only some elements in ω go to infinity, the number of limiting partitions is between those two extremes. Theorem 6 gives the number of limiting partitions.

Theorem 6. *Let $\pi \sim SP(\mu, \omega, \sigma, \psi, p_b)$, with $p_b(\pi) > 0$ for all possible π and $\omega = \omega \times (s_1, \dots, s_n)$, where s_i is either 0 or 1 and $\psi \in (0, 1)$. Let $a = n - \sum_{i=1}^n s_i$ be the number of items with shrinkage equal to zero. Let b be the number of clusters in μ having at least one item with $s = 1$. As $\omega \rightarrow \infty$, the number of limiting partitions in the SP distribution is $B(a, b)$ —an extension of the Bell numbers from Section 3.2.*

4.3 Prior Elicitation for Shrinkage and Grit Parameters

The previous subsections investigated the effects as elements of the shrinkage vector ω go to infinity and, when the number of items n permits exhaustive enumeration, the effects for finite values of ω . More generally, the effect of a particular shrinkage value (e.g., $\omega = 4$) will depend on other factors, such as the sample size n , the anchor partition μ , and the grit ψ . When enumeration is not feasible, we recommend simulation when eliciting priors on (or fixed values for) the shrinkage and grit parameters. We suggest specifying a two-dimensional grid of values for the shrinkage and grit parameters and then sampling from the SP distribution under each combination of values. We then recommend computing, for example, Monte Carlo estimates of the total variation distance, the expectation of the Rand index, and the expectation of the cluster entropy — defined as the negation of the sum of the relative cluster sizes times the natural logarithm of the relative cluster sizes — for each combination of shrinkage and grit values. The modeler can pick priors for shrinkage and grit values that are compatible with *a priori* beliefs for these quantities. We demonstrate these

ideas in Appendix E.

5 Dependent Random Partitions

5.1 Hierarchically-Dependent Random Partitions

Over the past several decades, Bayesian hierarchical models have been used extensively with a great deal of success. Dependence among datasets can be induced between similar populations by placing a common prior distribution on parameters of interest, e.g., means and variances, and then placing a hyperprior distribution on the hyperparameters of the common prior distribution. Using our SP distribution, these same principles can be applied to dependent partitions. Specifically, consider T separate collections of data, each with the same items to be clustered, and let $\boldsymbol{\pi}_1, \dots, \boldsymbol{\pi}_T$ be the latent partitions. We can “borrow strength” in the estimation of these partitions through the following hierarchical model:

$$\boldsymbol{\pi}_t \mid \boldsymbol{\mu} \sim \text{SP}(\boldsymbol{\mu}, \boldsymbol{\omega}, \boldsymbol{\sigma}_t, \psi, p_b), \quad \boldsymbol{\mu} \sim p(\boldsymbol{\mu}). \quad (8)$$

Any choice could be made for $p(\boldsymbol{\mu})$, e.g., a CRP or an SP with a “best guess” anchor. There are likewise many choices for p_b . MCMC techniques can be used for posterior inference on hyperparameters because the normalizing constant of the SP distribution is available.

The default choice for the shrinkage parameter might be $\boldsymbol{\omega} = \omega \times (1, \dots, 1)$ with a prior on the scalar ω . A more sophisticated prior could easily be adapted, such as, $\boldsymbol{\omega} = \omega \cdot \boldsymbol{s}_t$, with $s_i \geq 0$. Here s_i would permit each partition to have varying degrees of dependence among the collection of the T partitions. The point is that the degree of dependence among $\boldsymbol{\pi}_1, \dots, \boldsymbol{\pi}_T$ is governed by the shrinkage parameter ω . As with typical Bayesian hierarchical models, the model in (8) allows the extremes of independence and exact equality among the partitions $\boldsymbol{\pi}_1, \dots, \boldsymbol{\pi}_T$ by setting $\omega = 0$ or $\omega \rightarrow \infty$, respectively.

The hierarchy shown in (8) using the SP distribution can be expanded upon. For example, while analyzing neuroimaging data, [Song et al. \(2023\)](#) generalizes our approach. In

particular, they use an early version of our SP distribution in an innovative model to simultaneously cluster in two domains, namely, bi-clustering subjects and conditions. Additionally, an emerging concept in the partition literature is that of *multi-view* data (Duan, 2020; Franzolini et al., 2023; Dombowsky and Dunson, 2023). Our hierarchical framework naturally allows for different data types (perhaps some low-dimensional and others high-dimensional) to share information using partitions with a common latent partition.

5.2 Temporally-Dependent Random Partitions

Modeling dependent partitions over time is also very natural using our SP distribution. Again, assume we have partitions $\boldsymbol{\pi}_1, \dots, \boldsymbol{\pi}_T$ for the same items over time. Recently Page et al. (2022) presented a model to induce temporal dependence in partitions. They argue that dependency should be placed directly on the partitions, as opposed to the approach in much of the literature which attempts to induce dependence on random measures. We follow Page et al. (2022)’s philosophy and model dependence directly on the partitions using our SP distribution. A basic time-dependent model is:

$$\boldsymbol{\pi}_t \mid \boldsymbol{\pi}_{t-1} \sim \text{SP}(\boldsymbol{\pi}_{t-1}, \boldsymbol{\omega}, \boldsymbol{\sigma}_t, \psi, p_b), \quad \boldsymbol{\pi}_1 \sim p(\boldsymbol{\pi}_1), \quad (9)$$

for $t = 2, \dots, T$. When data are evenly spaced in time, we envision setting $\boldsymbol{\omega} = \omega \times (1, \dots, 1)$ with ω a common parameter over time. However, unlike Page et al. (2022), our framework is not restricted to data analysis involving equally-spaced time points. For example, the model is easily modified by parameterizing the shrinkage to be time-dependent, e.g., $\boldsymbol{\omega}_t = \frac{\omega}{d_t} \times (1, \dots, 1)$, where d_t is the difference in time between time t and time $t - 1$.

6 Empirical Application: Return to Education

In this section, we illustrate various uses of our SP distribution, demonstrate the dependent partition models from the previous section, and compare results from related partition

distributions. Consider a regression model studying the relationship between earnings and education attainment. The data were obtained from IPUMS CPS (Flood et al., 2023). In March of each year, a cross-section of individuals from the 50 United States and the District of Columbia (D.C.) are surveyed regarding their employment and demographic information. Data with harmonized variables are available from the years 1994 to 2020. Applying sensible filters for our application (e.g., only including working individuals) yields 139,555 observations. For simplicity, sampling weights are ignored for this demonstration.

Let \mathbf{y}_{it} be the vector of the natural logarithm of the average hourly earnings for individuals in state $i = 1, \dots, n$ ($n = 51$) in year $t = 1, \dots, T$ (with $t = 1$ corresponding to the year 1994 and $T = 27$). Let \mathbf{X}_{it} be a matrix of covariates containing a column of ones for the intercept and the following mutually-exclusive dummy variables related to educational attainment: high school graduate, some college, or at least a bachelors degree. The matrix \mathbf{Z}_{it} consists of non-education related covariates: age, age², hours worked weekly (weeklyhrs), weeklyhrs², and the following dummy variables: male, white, Hispanic, in a union, and married. We consider the regression model $\mathbf{y}_{it} = \mathbf{X}_{it}\boldsymbol{\beta}_{it} + \mathbf{Z}_{it}\boldsymbol{\gamma}_t + \boldsymbol{\epsilon}_{it}$, where the elements of $\boldsymbol{\epsilon}_{it}$ are independent and identically distributed normal with mean zero and precision τ_t . Conditional independence is assumed across states and years. Note that $\boldsymbol{\gamma}_t$ and τ_t lack a subscript i and are therefore common across all states. For a quick reference to the notation, we refer readers to Table 2 in Appendix C.

Interest lies especially in estimating the state-year specific regression coefficients $\boldsymbol{\beta}_{it}$ regarding educational attainment. Some state-year combinations have sufficient data (e.g., California has at least 497 observations per year), but some have limited data (e.g., D.C. has a year with only 20 observations) such that estimating $4+9+1 = 14$ parameters would be very imprecise. One solution is to combine data from small states, although such combinations may be *ad hoc*. Instead, in a given year t , we obtain parsimony and flexibility by postulating that the states are clustered by ties among $\boldsymbol{\beta}_{it}$ for $i = 1, \dots, n$. Let $\boldsymbol{\pi}_t = (\pi_{1t}, \dots, \pi_{nt})$ be

the clustering induced by these ties, where $\pi_{it} = \pi_{jt}$ if and only if $\beta_{it} = \beta_{jt}$. For notational convenience, we label the first item 1, use consecutive integers $1, \dots, q_t$ for the unique cluster labels in $\boldsymbol{\pi}_t$, and let $\beta_{1t}^*, \dots, \beta_{q_t t}^*$ be the unique values for the regression coefficients. Let \mathbf{X}_{ct} be the matrices obtained by vertically stacking the matrices \mathbf{X}_{it} for all i such that $\pi_{it} = c$. Likewise, \mathbf{Z}_{ct} is obtained by vertically stacking \mathbf{Z}_{it} when $\pi_{it} = c$ and let \mathbf{y}_{ct} be the vector obtained by concatenating \mathbf{y}_{it} for all i such that $\pi_{it} = c$.

The joint sampling model for data $\mathbf{y}_{1t}, \dots, \mathbf{y}_{nt}$ is:

$$p(\mathbf{y}_{1t}, \dots, \mathbf{y}_{nt} \mid \boldsymbol{\pi}_t, \beta_{1t}^*, \dots, \beta_{q_t t}^*, \boldsymbol{\gamma}_t, \tau_t) = \prod_{c=1}^{q_t} p(\mathbf{y}_{ct} \mid \beta_{ct}^*, \boldsymbol{\gamma}_t, \tau_t), \quad (10)$$

$$\text{with } \mathbf{y}_{ct} \mid \beta_{ct}^*, \boldsymbol{\gamma}_t, \tau_t \sim \text{N}(\mathbf{X}_{ct}\beta_{ct}^* + \mathbf{Z}_{ct}\boldsymbol{\gamma}_t, \tau_t \mathbf{I}), \quad (11)$$

where \mathbf{I} is an identity matrix and $\text{N}(\mathbf{a}, \mathbf{B})$ represents a multivariate normal distribution with mean \mathbf{a} and precision matrix \mathbf{B} .

We use the following joint prior distribution for the other parameters as the product of independent distributions. The precisions τ_1, \dots, τ_T in the sampling distribution are *iid* gamma with shape $a_\tau = 1/0.361^2$ and rate $b_\tau = 1$, making the prior expected standard deviation equal a preliminary guess of 0.361 obtained by exploratory data analysis. The regression coefficient vector $\boldsymbol{\gamma}_t$ has a normal prior distribution with mean $\boldsymbol{\mu}_\gamma = \mathbf{0}$ and precision $\boldsymbol{\Lambda}_\gamma = \mathbf{I}$. Based on preliminary explorations using ordinary least squares, the priors for the cluster-specific regression coefficients $\beta_{1t}^*, \dots, \beta_{q_t t}^*$ are independent and identically distributed normal with mean $\boldsymbol{\mu}_\beta = (1.46, 0.15, 0.24, 0.41)'$ and precision $\boldsymbol{\Lambda}_\beta$ is $100\mathbf{I}$.

As the pmf of the SP distribution is available in closed form, the full suite of standard MCMC algorithms are available to sample from the posterior distribution. Our approach for updating the cluster labels is a Pólya urn Gibbs sampler based on [Neal \(2000\)](#)'s Algorithm 8. One caveat is that the SP distribution is not exchangeable, so its full pmf — or, at least, the part involving the current item and any item allocated after it according to the permutation $\boldsymbol{\sigma}$ — must be computed. Specific MCMC details are given in [Appendix C](#).

Recall that we have T years with partitions $\boldsymbol{\pi}_1, \dots, \boldsymbol{\pi}_T$. We now discuss three specifications for the joint prior distribution for $\boldsymbol{\pi}_1, \dots, \boldsymbol{\pi}_T$. We first consider independent random partitions in Section 6.1 and use this model as a means to compare the SP distribution with the CPP and the LSP. We then consider hierarchically and temporally dependent random partitions in Sections 6.2 and 6.3, respectively.

6.1 Application Using Independent Partitions

In this section, we consider various prior distributions for $\boldsymbol{\pi}_1, \dots, \boldsymbol{\pi}_T$ of the form $p(\boldsymbol{\pi}_1, \dots, \boldsymbol{\pi}_T) = \prod_{t=1}^T p(\boldsymbol{\pi}_t)$. One’s best guess for an unknown partition $\boldsymbol{\pi}_t$ may be the partition given by the four US Census Regions, shown in Figure 3 of Appendix D. Indeed, at one extreme, one may wish to fix $\boldsymbol{\pi}_t$ to be these regions, effectively using a point-mass distribution $p(\boldsymbol{\pi}_t)$ on the regions. At the other extreme, one may disregard the regions and specify, for example, that $\boldsymbol{\pi}_t \sim \text{CRP}(1)$ or $\boldsymbol{\pi}_t \sim \text{JLP}(1)$.

We entertain compromises between these extremes. In this subsection, we fix $\boldsymbol{\mu}$ to be the anchor partition given by the U.S. Census Bureau regions and consider several partition distributions informed by this “best guess” partition $\boldsymbol{\mu}$. Specifically, we consider the shrinkage partition (SP) distribution, the centered partition process (CPP), and the location-scale partition (LSP) distribution. Recall that the normalizing constant is not known for the CPP and hence the shrinkage value ω must be fixed when using standard MCMC methods. In this subsection, for the sake of comparison with the CPP, we also fix the shrinkage for the SP and LSP. The specifics of how ω influences each distributional family differ and it is not clear how to calibrate an ω for each distributional family such that the influence of $\boldsymbol{\mu}$ is commensurate. Instead, we consider a distribution-specific grid of values for ω and only present results for the best-fitting model of each distributional family. We show results for models using the following prior partition distributions: i. “Location-Scale Partition”: $\boldsymbol{\pi}_t \sim \text{LSP}(\boldsymbol{\mu}, \omega = 3990.81)$ using our permutation modification to make the analysis invariant to observation

order, ii. “Centered Partition Process w/ VI Loss”: $\pi_t \sim \text{CPP}(\boldsymbol{\mu}, \omega = 30, \text{VI}, \text{CRP}(1))$, iii. “Centered Partition Process w/ Binder Loss”: $\pi_t \sim \text{CPP}(\boldsymbol{\mu}, \omega = 500, \text{Binder}, \text{CRP}(1))$, iv. “Shrinkage Partition – Common”: $\pi_t \sim \text{SP}(\boldsymbol{\mu}, \boldsymbol{\omega}, \psi = 0.02, \text{CRP}(1))$ with $\boldsymbol{\omega} = (5, \dots, 5)$, v. “Shrinkage Partition – Idiosyncratic”: $\pi_t \sim \text{SP}(\boldsymbol{\mu}, \boldsymbol{\omega}, \psi = 0.02, \text{CRP}(1))$ with $\boldsymbol{\omega} = 5 \times (a_1, \dots, a_n)$ in which $a_i = 1$ for all states except $a_i = 1/5$ for Maryland, Delaware, District of Columbia, Montana, North Dakota, and South Dakota. These states with $a_i = 1/5$ are on the borders of regions and it is reasonable to be less confident in the allocation to their particular region in the anchor partition $\boldsymbol{\mu}$. Note that, for the sake of comparison, we fix the concentration parameter at $\alpha = 1$ for the CRP baseline distribution. In practice, one might treat α as random when using our SP distribution since it has a tractable normalizing constant.

To assess fit, we performed 10-fold cross validation as follows. The dataset was divided into 10 equally-sized, mutually-exclusive, and exhaustive shards (subsets). For each fold, one of the 10 shards was held out as the test dataset for a model fit with the other 9 shards. For each fold, 55,000 MCMC iterations were run, the first 5,000 were discarded as burn-in, and 1-in-10 thinning was applied for convenience. For each MCMC iteration, the permutation $\boldsymbol{\sigma}_t$ received ten Metropolis update attempts based on uniformly sampling ten items from $\boldsymbol{\sigma}_t$ and randomly shuffling them. We computed the out-of-sample log-likelihood, defined as the sum of the Monte Carlo estimate of the expectation of the log-likelihood contribution for each observation when it was part of the held-out shard. We then divide this sum by the sample size and multiply by 1,000,000 (for convenience) to get a per-unit fit score, where larger values indicate better out-of-sample fit. To aid in comparisons, we show “relative fit scores” with reference to the CRP(1), that is, the fit score for a particular model minus that of the CRP(1). Results are summarized in Table 1, where the models are ordered with the best performing at the top. Each of the SP, CPP, and LSP prior improve upon the one extreme of the CRP (which ignores the region information) and the other extreme

Prior Partition Distribution	Relative Fit	Time
Shrinkage Partition Distribution – Idiosyncratic	2,448	60.2
Shrinkage Partition Distribution – Common	1,854	60.3
Centered Partition Process w/ VI Loss	1,842	32.6
Location-Scale Partition	1,272	97.1
Centered Partition Process w/ Binder Loss	781	35.9
Fixed Partition of μ	620	25.7
Chinese Restaurant Process	0	27.2
Saturated Regression Model	-10,221	

Table 1: Monte Carlo estimates of our relative fit score, defined as the mean out-of-sample log-likelihood (based on 10-fold cross validation) minus that of the CRP(1), times 1,000,000. Larger values indicate better fit. The largest margin of error for 95% Monte Carlo confidence intervals is 14 units. The elapsed time for each model, in minutes, is also shown.

of fixing the partition at the anchor partition μ defined by the regions. In particular, the model with our SP prior performs 2,448 units better than the model using the CRP prior, an improvement that we put in context in Section 6.3. Elapsed time for the full data analysis for each model using single-threaded code is included in the table. All the timing metrics in this paper were computed on a server with 256 GB of RAM and with dual Intel Xeon Gold 6438Y+ CPUs.

To consider a simple alternative model for the sake of benchmarking, Table 1 also contains the relative fit score of a saturated regression model having covariates obtained by: i. interacting 27 year dummy variables with the nine covariates in the \mathbf{Z} matrix and ii. interacting the 27 year dummy variables, 51 state dummy variables, and the four covariates in the \mathbf{X} matrix. (About a dozen three-way interactions could not be estimated due to limitations of the data.) The saturated regression model does not permit the borrowing of strength (and assumes homoskedastic errors across years), leading to substantially worse out-of-sample performance.

6.2 Application Using Hierarchically-Dependent Partitions

The model in the previous subsection assumed *a priori* independence among the partitions $\boldsymbol{\pi}_1, \dots, \boldsymbol{\pi}_T$. Note that we are repeatedly clustering the same items and one might expect an improvement by allowing the “borrowing of strength” in partition estimation. In this subsection, we demonstrate the Bayesian hierarchical model presented in Section 5.1. This illustrates that, in a very intuitive way, dependent partition models can be formulated in the same way as other Bayesian hierarchical models. We show that our model produces a large improvement in the fit score when compared to the models in the previous subsection.

Our hierarchical model uses the sampling model as defined in (10) and (11) and a hierarchical prior for the partitions $\boldsymbol{\pi}_1, \dots, \boldsymbol{\pi}_T$ given in (8), with $\boldsymbol{\mu} \sim \text{SP}(\boldsymbol{\rho}_r, \boldsymbol{\omega}_0, \boldsymbol{\sigma}_0, \psi_0, \text{CRP}(1))$, $\boldsymbol{\omega} = \omega \times (1, \dots, 1)$ and $\omega \sim \text{Gamma}(5, 1)$, $\boldsymbol{\sigma}_t$ having a discrete uniform distribution, ψ having a uniform prior on the unit interval, and baseline distribution p_b being $\text{CRP}(1)$. For the hyperparameters of the SP prior on $\boldsymbol{\mu}$, the anchor $\boldsymbol{\rho}_r$ is the partition defined by the US Census Bureau regions, we set $\boldsymbol{\omega}_0 = \omega_0 \times (a_1, \dots, a_n)$ using a_i values from Section 6.1 and place a $\text{Gamma}(5, 1)$ prior on ω_0 , we assume a uniform prior on $\boldsymbol{\sigma}_0$, and we place a uniform prior on the unit interval for the grit parameter ψ_0 . Of course, other distributional choices could be made for $p(\boldsymbol{\mu})$ and p_b . In any case, inference is straightforward since standard MCMC techniques are available when using the SP distribution due to its tractable normalizing constant. These priors for the shrinkage and grit parameters were chosen as outlined in Section 4.3 and demonstrated in Appendix E.

The permutations were updated using a Metropolis step that was applied 10 times per MCMC iteration for each permutation, with each randomly proposing to shuffle 5 items. The acceptance rate for an individual update was 7%. The single-core runtime each Markov chain was approximately 103 minutes; about 52% of that time was used to update the anchor partition, 3% on the shrinkage and grit parameters, 5% on the permutation parameters, and the remaining 40% on the other year-specific parameters.

To compare models, we again use the same 10-fold out-of-sample fit measure with the same number of samples, burn-in, and thinning as in the previous subsection. We repeated the whole exercise ten times with randomly selected starting values and then combined the samples after burn-in. The relative fit score was 3,539 (with margin of error 109 for a 95% confidence interval), a substantial improvement of about 1,091 units from the best model fit from the independence models in Section 6.1.

6.3 Application Using Temporally-Dependent Partitions

We demonstrated in Section 6.2 the hierarchically-dependent partition model defined in Section 5.1. This model greatly improved results over the independent models in Section 6.1, however, the hierarchical structure did not capture the intuition that two adjacent years are likely more dependent than two years that are far apart. The data in this example are a time series for $t = 1, \dots, T$, and thus an autoregressive model in time for π_1, \dots, π_T is natural. We now demonstrate that the temporal model in Section 5.2 improves upon the results of the hierarchical model.

We follow the outline of Section 5.2 and use the same sampling model, priors on the shrinkage and grit parameters, number of posterior samples, burn-in, thinning, 10-fold cross validation, etc. as in Section 6.2. We assume $\pi_1 \sim \text{SP}(\rho_r, \omega_0, \sigma_0, \psi_0, \text{CRP}(1))$, with anchor ρ_r defined by the census regions, $\omega_0 = \omega_0 \times (a_1, \dots, a_n)$ using a_i values from Section 6.1 and placing a Gamma(5, 1) prior on ω_0 , a uniform prior on σ_0 , and a uniform prior on the unit interval for the grit parameter ψ_0 . The acceptance rate for a permutation update was 15%. The single-core runtime of each Markov chain was approximately 165 minutes; about 2% of the that time was used to update the shrinkage and grit parameters, 2% on the permutation parameters, and the remaining 96% on the other year-specific parameters.

Figure 2 helps visualize the dependence among the yearly partitions π_1, \dots, π_T . Each plot is a 27×27 grid with the (i, j) cell showing the posterior expectation of the Rand index

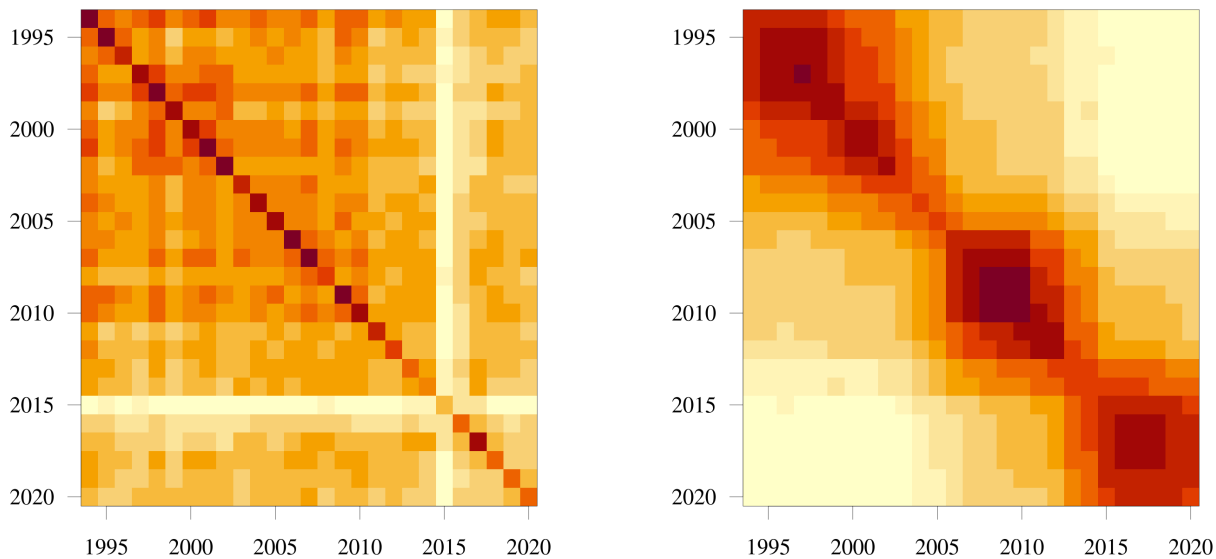


Figure 2: The posterior expected Rand index for years 1994 to 2020. Darker colors indicate greater partition agreement. The left plot is for the independent model from Section 6.1 and the right plot is for our model for temporally-dependent random partitions.

(RI) between two randomly selected partitions from years i and j . More agreement in the partitions, i.e., larger RI value, are shown in darker colors in the plots. The left plot is for the independent CRP model in Section 6.1 and the right plot is for the time-dependent model. There is a stark contrast between the plots of two models, with the temporally-dependent model demonstrating the anticipated temporal-dependence in neighboring years which decays over time (i.e., moving away from the diagonal).

We again use the same 10-fold out-of-sample fit measure with the same number of samples, burn-in, and thinning and repeated the whole exercise ten times. The relative fit score was $5,000 \pm 64$, which is a substantial improvement of about 1,461 units from the hierarchical model in Section 6.2 and 2,552 units better than the best model fit from the independence models in Section 6.1.

To explore the scientific significance of the improvement in out-of-sample fit, we considered two approaches. First, we randomly deleted 40% and 50% of the observations from each training dataset in our 10-fold cross validation scheme, refit exactly the same model

as described in this section, and found that the relative fit score was 1,176 and -1,053, respectively. We conclude that, for this study, one could reduce the required sample size by about 45% — and therefore save significantly in the cost of data acquisition — while still achieving about the same performance as the CRP(1) model with all the data. Second, we removed the “married” dummy variable, refit the model (with all of the observations), and found the relative fit score was 1,026. Likewise, we instead removed both the “white” and “Hispanic” dummy variables, refit the model, and found the relative fit was -1,780. We conclude that using our model with temporally-dependent partitions adds an approximate performance boost of an additional covariate to the CRP(1) model, with the importance of that hypothetical covariate lying somewhere between “married” or the pair “white” and “Hispanic”. In practice, analysts would always want to include these demographic dummy variables and would always want to use all the available data. This exercise merely demonstrates the scientific significance of using our temporally-dependent partitions model over a simpler model that does not capture partition dependence. Likewise, we conclude that our hierarchical model and independent model using the SP distribution also both have scientifically significant (albeit more modest) gains.

7 Scalability

The added flexibility of the SP distribution in accommodating a “best-guess” partition or in modeling dependent partitions comes at a computational cost. We first consider scalability in the number of time points T . We reran the dependent models in Section 6 with data from 1994-2002 ($T = 9$), 1994-2011 ($T = 18$), 1994-2020 ($T = 27$), 1994-2020 with 2020 down to 2011 ($T = 36$), 1994-2020 with 2020 down to 2002 ($T = 45$), 1994-2020 with 2020 down to 1994 ($T = 54$). The elapsed time (using one CPU core) to fit the hierarchical model ranged from 0.79 hours ($T = 9$) to 2.89 hours ($T = 54$), with a simple linear regression (SLR) model in T explaining almost $R^2 = 99\%$ of the variation in the elapsed time. Likewise, the time

to fit the temporal model ranged from 1.14 hours ($T = 9$) to 4.28 hours ($T = 54$), with $R^2 = 98\%$. Thus both the hierarchical and the temporal models appear to scale linearly with T .

We also investigated the scalability in the number of clusters. Consider the data from 1994 and the model from Section 6.1. By varying the concentration parameter α of the CRP(α) baseline distribution in the SP distribution, we generated posterior samples for which the average number of clusters ranged from 3.6 ($\alpha = 0.01$) to 14.4 ($\alpha = 10$). The elapsed time was also recorded and a SLR of elapsed time on the average number of clusters showed an adequate fit to the data ($R^2 = 95\%$), suggesting that the elapsed time is approximately linear in the number of clusters.

While these models scale very well in the number of time points T and number of clusters, scaling in the number of items n is more challenging. Recall that all models to this point have clustered $n = 51$ states. To investigate scalability in n , we timed the SP model in Section 6.1 using data from 1994 ($n = 51$), data from 1994-1995 treating states in different years as distinct items ($n = 102$), data from 1994-1996 ($n = 153$), ..., data from 1994-2022 ($n = 1,377$). The elapsed time (using one CPU core) ranged from just over a minute ($n = 51$) to just under 28 hours ($n = 1,377$), and we found that the square root of the elapsed time was linear in the number of items n , with a SLR having $R^2 = 99.9\%$. Thus the SP model appears to scale quadratically in n . In contrast, the elapsed time for the CRP model with $n = 1,377$ was about 14 minutes. Clearly the SP model is not practical for tens of thousands of items, but we have demonstrated feasibility for at least $n = 1,377$ items. We note, that one approach to reducing the computational cost may be to select a baseline distribution that favors a smaller number of clusters, for example, the CRP with a low mass parameter or a distribution with repulsive atoms similar to [Beraha et al. \(2022\)](#).

8 Discussion

We introduced a random partition distribution which shrinks a partition distribution p_b to an anchor partition $\boldsymbol{\mu}$ according to a shrinkage parameter $\boldsymbol{\omega}$. The primary motivation for this new partition distribution was to provide a straightforward mechanism to implement dependent partition models. We discussed and demonstrated the advantages of our SP distribution relative to the CPP and LSP. We proved several intuitive properties of the SP distribution. We then developed models for dependent partitions and demonstrated their performance in an empirical study. We showed that adding dependency among related partitions, first using a hierarchical framework followed by time-series structure, improves the model performance quite dramatically. Appendix E shows that the SP distribution behaves as one would expect in a typical Bayesian model, improving estimation when prior assumptions are met, worsening estimation when prior assumptions are bad, and yielding to the data as the sample size increases.

References

- Airoldi, E. M., T. Costa, F. Bassetti, F. Leisen, and M. Guindani (2014). Generalized species sampling priors with latent beta reinforcements. Journal of the American Statistical Association 109(508), 1466–1480.
- Argiento, R., A. Cremaschi, and M. Vannucci (2020). Hierarchical normalized completely random measures to cluster grouped data. Journal of the American Statistical Association 115(529), 318–333.
- Beraha, M., R. Argiento, J. Møller, and A. Guglielmi (2022). MCMC computations for Bayesian mixture models using repulsive point processes. Journal of Computational and Graphical Statistics 31(2), 422–435.

- Betancourt, B., J. Sosa, and A. Rodríguez (2022). A prior for record linkage based on allelic partitions. Computational Statistics & Data Analysis 172, 107474.
- Binder, D. A. (1978, 04). Bayesian cluster analysis. Biometrika 65(1), 31–38.
- Blei, D. M. and P. I. Frazier (2011). Distance dependent chinese restaurant processes. Journal of Machine Learning Research 12(8), 2461–2488.
- Camerlenghi, F., A. Lijoi, P. Orbanz, and I. Pr ünster (2019). Distribution theory for hierarchical processes. The Annals of Statistics 47(1), 67–92.
- Casella, G., E. Moreno, F. J. Girón, et al. (2014). Cluster analysis, model selection, and prior distributions on models. Bayesian Analysis 9(3), 613–658.
- Dahl, D. B., R. Day, and J. W. Tsai (2017). Random partition distribution indexed by pairwise information. Journal of the American Statistical Association 112(518), 721–732.
- Dahl, D. B., D. J. Johnson, and P. Müller (2022). Search algorithms and loss functions for Bayesian clustering. Journal of Computational and Graphical Statistics 31(4), 1189–1201.
- Dahl, D. B., R. L. Warr, and T. P. Jensen (2021). Discussion: Centered partition processes: Informative priors for clustering. Bayesian Analysis 16(1), 333–338.
- Dombowsky, A. and D. B. Dunson (2023). Product centered Dirichlet processes for dependent clustering. arXiv preprint arXiv:2312.05365.
- Duan, L. L. (2020). Latent simplex position model: High dimensional multi-view clustering with uncertainty quantification. Journal of Machine Learning Research 21(38), 1–25.
- Ewens, W. J. (1972). The sampling theory of selectively neutral alleles. Theoretical Population Biology 3(1), 87–112.

- Flood, S., M. King, R. Rodgers, S. Ruggles, J. R. Warren, and M. Westberry (2023). Integrated Public Use Microdata Series, Current Population Survey: Version 11.0 [dataset]. Minneapolis, MN: IPUMS.
- Franzolini, B., M. De Iorio, and J. Eriksson (2023). Conditional partial exchangeability: a probabilistic framework for multi-view clustering. arXiv preprint arXiv:2307.01152.
- Ghosal, L. and A. van der Vaart (2017). Fundamentals of Bayesian Nonparametric Inference. Cambridge University, Press.
- Hartigan, J. A. (1990). Partition models. Communications in Statistics-Theory and Methods 19(8), 2745–2756.
- Jensen, S. T. and J. S. Liu (2008). Bayesian clustering of transcription factor binding motifs. Journal of the American Statistical Association 103(481), 188–200.
- Meilă, M. (2007). Comparing clusterings—an information based distance. Journal of Multivariate Analysis 98(5), 873–895.
- Müller, P., F. Quintana, and G. L. Rosner (2011). A product partition model with regression on covariates. Journal of Computational and Graphical Statistics 20(1), 260–278.
- Müller, P., F. Quintana, and G. Rosner (2004, 07). A method for combining inference across related nonparametric Bayesian models. Journal of the Royal Statistical Society Series B: Statistical Methodology 66(3), 735–749.
- Neal, R. M. (2000). Markov chain sampling methods for Dirichlet process mixture models. Journal of Computational and Graphical Statistics 9(2), 249–265.
- Paganin, S., A. H. Herring, A. F. Olshan, and D. B. Dunson (2021). Centered partition processes: Informative priors for clustering (with discussion). Bayesian Analysis 16(1), 301–370.

- Paganin, S., G. L. Page, and F. A. Quintana (2023). Informed random partition models with temporal dependence. arXiv preprint arXiv:2311.14502.
- Page, G. L. and F. A. Quintana (2016). Spatial product partition models. Bayesian Analysis 11(1), 265–298.
- Page, G. L., F. A. Quintana, and D. B. Dahl (2022). Dependent modeling of temporal sequences of random partitions. Journal of Computational and Graphical Statistics 31(2), 614–627.
- Park, J.-H. and D. B. Dunson (2010). Bayesian generalized product partition model. Statistica Sinica 20(3), 1203–1226.
- Pitman, J. (1995). Exchangeable and partially exchangeable random partitions. Probability Theory and Related Fields 102(2), 145–158.
- Pitman, J. and M. Yor (1997). The two-parameter Poisson-Dirichlet distribution derived from a stable subordinator. The Annals of Probability 25(2), 855–900.
- Rastelli, R. and N. Friel (2018, Nov). Optimal Bayesian estimators for latent variable cluster models. Statistics and Computing 28(6), 1169–1186.
- Smith, A. N. and G. M. Allenby (2020). Demand models with random partitions. Journal of the American Statistical Association 115(529), 47–65.
- Song, Z., W. Shen, M. Vannucci, A. Baldizon, P. M. Cinciripini, F. Versace, and M. Guindani (2023). Clustering computer mouse tracking data with informed hierarchical shrinkage partition priors. pre-publication manuscript.
- Wade, S. and Z. Ghahramani (2018). Bayesian cluster analysis: Point estimation and credible balls (with discussion). Bayesian Analysis 13(2), 559–626.

Appendix A An Extension to the Bell Number

The n^{th} Bell number provides the number of possible unique partitions of n items. Here we construct an extension of the Bell numbers enumerating how many unique partitions are possible when allocating a items to b existing subsets. We denote these numbers as $B(a, b)$ where a and b must be nonnegative integers. We start with the trivial cases. First, by definition $B(0, 0) \equiv 1$. If there are a items to allocate and $b = 0$ (i.e., there are no existing subsets) then we have the standard Bell numbers $B(a, 0) \equiv B(a)$. Another trivial case is when there are no items to allocate (i.e., $a = 0$) with b existing subsets then we have $B(0, b) \equiv 1$. It is straightforward to see that $B(1, b) = b + 1$, since there are b current subsets and the one item to be allocated could go to the b existing subsets or a new subset.

This extension to the Bell numbers also follow a similar recursive formula to that of the Bell numbers. We have:

$$B(a, b + 1) = \sum_{i=0}^a \binom{a}{i} B(i, b). \quad (12)$$

To show this relationship is true we make the following argument. First assume $B(a, b)$ is the number of possible unique partitions when allocating a items and b subsets already exist. We are now assuming we have $b + 1$ existing subsets before allocating the a items. That extra subset must be contained in exactly one of the following cases:

- None of those a items are added to that subset: there are $B(a, b)$ unique partitions in this case
- One of those a items are added to that subset: there are $\binom{a}{1} B(a - 1, b)$ unique partitions in this case
- Two of those a items are added to that subset: there are $\binom{a}{2} B(a - 2, b)$ unique partitions in this case
- \vdots
- All a of those items are added to that subset: there are $\binom{a}{a} B(0, b)$ unique partitions in

this case

Recalling that $\binom{a}{i} = \binom{a}{a-i}$ and summing all the possible cases in reverse order, we have that $B(a, b + 1) = \sum_{i=0}^a \binom{a}{i} B(i, b)$.

A useful recurrence formula for these numbers are:

$$B(a + 1, b) = b B(a, b) + B(a, b + 1). \tag{13}$$

We can show this formula is correct using the following logic. Consider all possible ways to allocate the $(a + 1)^{\text{th}}$ item (before the other a items have been allocated to a subset). There are two main cases:

- It goes to one of the existing b subsets
- It goes to a new singleton subset

If the $(a + 1)^{\text{th}}$ item goes to one of the existing subsets then there are $B(a, b)$ ways to allocate the other items. However, we need to multiply that by the number of ways the $(a + 1)^{\text{th}}$ item can be allocated to the preexisting subsets. Thus for the first case we have $b B(a, b)$ possible partitions.

If the $(a + 1)^{\text{th}}$ item goes to a new singleton subset, then there are $b + 1$ existing subsets in which to allocate a items, or $B(a, b + 1)$. These two cases comprise all possibilities and give the number for adding a new item to allocate.

Note that (13) is especially useful in generating these numbers.

Appendix B Proofs and Properties

B.1 Proof of Theorem 1

Theorem 1: Let ρ_1 be the partition with all n items assigned to a single cluster, ρ_n be the partition with n items each assigned to a unique cluster, $\pi \sim SP(\boldsymbol{\mu}, \boldsymbol{\omega}, \psi, p_b)$ with $p_b(\boldsymbol{\mu}) > 0$, and $\boldsymbol{\omega} = \omega \times (1, \dots, 1)$:

- a) if $\omega = 0$, then $\pi \sim p_b$. [Diffusion to the baseline dist'n]
- b) if $\psi \in (0, 1)$ then $\lim_{\omega \rightarrow \infty} Pr(\pi = \boldsymbol{\mu}) = 1$ [Anchor partition consistency]
- c) if $\psi \in (-\infty, 0)$ then $\lim_{\omega \rightarrow \infty} Pr(\pi = \rho_1) = 1$
- d) if $\psi \in (1, \infty)$ then $\lim_{\omega \rightarrow \infty} Pr(\pi = \rho_n) = 1$.

Proof:

For **part a)** this property is easily demonstrated by looking at the CAPF of the SP distribution and setting $\omega = 0$. Now the exponential term is equal to 1 and we are left with the CAPF of p_b .

For **part b)** under the conditions that $\pi = \boldsymbol{\mu}$, $\boldsymbol{\omega} = \omega \times (1, \dots, 1)$, and $0 < \omega < \infty$, the CAPF of the SP distribution reduces to:

$$\begin{aligned} \Pr_{\text{sp}}(\pi_{\sigma_k} = \mu_{\sigma_k} \mid \pi_{\sigma_1}, \dots, \pi_{\sigma_{k-1}}, \boldsymbol{\mu}, \boldsymbol{\omega}, \boldsymbol{\sigma}, \psi, p_b) &= \tag{14} \\ & \frac{\Pr_b(\pi_{\sigma_k} = \mu_{\sigma_k} \mid \pi_{\sigma_1}, \dots, \pi_{\sigma_{k-1}}) \times \exp\left(\frac{(1-\psi)\omega^2}{k-1} \sum_{j=1}^{k-1} \mathbb{I}\{\mu_{\sigma_j} = \mu_{\sigma_k}\}\right)}{\sum_{c \in \mathcal{S}} \Pr_b(\pi_{\sigma_k} = c \mid \pi_{\sigma_1}, \dots, \pi_{\sigma_{k-1}}) \times \exp\left(\frac{(\mathbb{I}\{\mu_{\sigma_k} = c\} - \psi)\omega^2}{k-1} \sum_{j=1}^{k-1} \mathbb{I}\{\mu_{\sigma_j} = c\}\right)} \end{aligned}$$

for $k = 2, \dots, n$ and where $\mathcal{S} = \{\mu_{\sigma_1}, \dots, \mu_{\sigma_{k-1}}, |\{\mu_{\sigma_1}, \dots, \mu_{\sigma_{k-1}}\}| + 1\}$. This can be justified since if $\pi = \boldsymbol{\mu}$ then $\mathbb{I}\{\pi_{\sigma_j} = c\} = \mathbb{I}\{\mu_{\sigma_j} = c\}$. Further, in the numerator, since $c = \mu_{\sigma_k}$ we have $\mathbb{I}\{\mu_{\sigma_j} = c\} = \mathbb{I}\{\mu_{\sigma_j} = \mu_{\sigma_k}\}$.

We are given that ψ is confined to the interval $(0, 1)$. For a fixed value of k , if c agrees with $\boldsymbol{\mu}$ (i.e., $\mathbb{I}\{\mu_{\sigma_j} = c\} = 1$) then the exponential term is positive and goes to infinity with

ω . If c does not agree with $\boldsymbol{\mu}$ (i.e., $\mathbb{I}\{\mu_{\sigma_j} = c\} = 0$) then the exponential term is negative and goes to 0 as $\omega \rightarrow \infty$. Thus for each k the CAPF forces the allocation to agree with $\boldsymbol{\mu}$ with probability 1 and, using the algebraic limit theorem, we have $\lim_{\omega \rightarrow \infty} \Pr(\boldsymbol{\pi} = \boldsymbol{\mu}) = 1$. For **part c)** we know $\psi \in (-\infty, 0)$. The expression in the exponential part of the SP's CAPF of (2) can be expressed as:

$$\frac{\omega^2}{k-1} \sum_{j=1}^{k-1} \mathbb{I}\{\pi_{\sigma_j} = c\} (\mathbb{I}\{\mu_{\sigma_j} = \mu_{\sigma_k}\} - \psi). \quad (15)$$

The value of $(\mathbb{I}\{\mu_{\sigma_j} = \mu_{\sigma_k}\} - \psi)$ will always be positive in this case. Since by definition $\pi_{\sigma_1} = 1$, the second item will be forced to be allocated with the first, i.e., Equation (15) will be infinite if $\pi_{\sigma_2} = 1$ and zero otherwise. The same will hold for each subsequent item allocation. Thus if $\psi \in (-\infty, 0)$ then $\lim_{\omega \rightarrow \infty} \Pr(\boldsymbol{\pi} = \boldsymbol{\rho}_1) = 1$.

For **part d)** we make a similar argument as in part c). If $\psi \in (1, \infty)$ then (15) will always be zero or negative. A partition that forces this part of the CAPF to always be zero will have positive probability mass as ω gets large. The partition $\boldsymbol{\rho}_n$ (each item is allocated to a unique cluster) is the only partition that matches that criterion since $\mathbb{I}\{\pi_{\sigma_j} = c\}$ will always be equal to 0. As items are sequentially allocated each item must go to its own cluster with probability 1, and no other partition has that property. Thus if $\psi \in (1, \infty)$ then $\lim_{\omega \rightarrow \infty} \Pr(\boldsymbol{\pi} = \boldsymbol{\rho}_n) = 1$. \square

In general, we recommend specifications of the SP distribution where $\psi \in (0, 1)$ because the distribution is consistent with the anchor partition as demonstrated in **part b)**. This is an ideal property for applications where the anchor partition is elicited as the prior clustering configuration and the intended interpretation of the shrinkage ω is a degree of compromise between the baseline p_b and the anchor partition $\boldsymbol{\rho}$. While $\psi \notin (0, 1)$ is a valid specification as implied in **part c)** and **part d)**, we urge caution interpreting the SP distribution parameters when consistency does not hold.

B.2 Proof of Theorem 2

Theorem 2: For any $\delta > 0$ and p_b such that $0 < p_b(\boldsymbol{\mu}) < 1$, if $\boldsymbol{\pi}_1 \sim SP(\boldsymbol{\mu}, \boldsymbol{\omega}, \psi, p_b)$ and $\boldsymbol{\pi}_2 \sim SP(\boldsymbol{\mu}, \boldsymbol{\omega} + \delta, \psi, p_b)$ with $\boldsymbol{\omega} = \omega \times (1, \dots, 1)$, $0 \leq \omega < \infty$ and $\psi \in (0, 1)$, then $Pr(\boldsymbol{\pi}_1 = \boldsymbol{\mu}) < Pr(\boldsymbol{\pi}_2 = \boldsymbol{\mu})$.

Proof:

Under the conditions that $\boldsymbol{\pi} = \boldsymbol{\mu}$, $\boldsymbol{\omega} = \omega \times (1, \dots, 1)$ and $0 < \omega < \infty$, the CAPF of the SP distribution reduces to (14). To streamline notation we let $d_k(c) = \sum_{j=1}^{k-1} \mathbb{I}(\mu_{\sigma_j} = c)/(k-1)$ and write $\Pr_b(\pi_{\sigma_k} = c \mid \pi_{\sigma_1}, \dots, \pi_{\sigma_{k-1}})$ as $\Pr_b(\pi_{\sigma_k} = c \mid \cdot)$. Thus the CAPF can be more compactly written as:

$$\frac{\Pr_b(\pi_{\sigma_k} = \mu_{\sigma_k} \mid \cdot) \exp(d_k(\mu_{\sigma_k})(1-\psi)\omega^2)}{\sum_{c \in \mathcal{S}} \Pr_b(\pi_{\sigma_k} = c \mid \cdot) \exp(d_k(c)(\mathbb{I}\{\mu_{\sigma_k} = c\} - \psi)\omega^2)}.$$

We want to show:

$$\begin{aligned} & \Pr_{\text{sp}}(\pi_{\sigma_k} = \mu_{\sigma_k} \mid \pi_{\sigma_1}, \dots, \pi_{\sigma_{k-1}}, \boldsymbol{\mu}, \boldsymbol{\omega} + \delta, \boldsymbol{\sigma}, \psi, p_b) \\ & \geq \Pr_{\text{sp}}(\pi_{\sigma_k} = \mu_{\sigma_k} \mid \pi_{\sigma_1}, \dots, \pi_{\sigma_{k-1}}, \boldsymbol{\mu}, \boldsymbol{\omega}, \boldsymbol{\sigma}, \psi, p_b) \end{aligned}$$

for $k = 2, \dots, n$ and that the inequality is strict for at least one k and $\boldsymbol{\sigma}$. This is equivalent to showing:

$$\begin{aligned} & \sum_{c \in \mathcal{S}} \Pr_b(\pi_{\sigma_k} = c \mid \cdot) \exp(d_k(c)(\mathbb{I}\{\mu_{\sigma_k} = c\} - \psi)\omega^2) \exp(d_k(\mu_{\sigma_k})(1-\psi)(\omega + \delta)^2) \\ & \geq \sum_{c \in \mathcal{S}} \Pr_b(\pi_{\sigma_k} = c \mid \cdot) \exp(d_k(c)(\mathbb{I}\{\mu_{\sigma_k} = c\} - \psi)(\omega + \delta)^2) \exp(d_k(\mu_{\sigma_k})(1-\psi)\omega^2) \end{aligned}$$

Before we drop the $\Pr_b(\pi_{\sigma_k} = c \mid \cdot)$ from consideration, recall that $0 < p_b(\boldsymbol{\mu}) < 1$, thus there must exist at least one $\boldsymbol{\sigma}$, k , and $c \neq \mu_{\sigma_k}$ such that $\Pr_b(\pi_{\sigma_k} = c \mid \cdot) > 0$. Now comparing the summands for each possible c , we see if $c = \mu_{\sigma_k}$ then the terms on each side of the inequality are equal. If $c \neq \mu_{\sigma_k}$ then we can reduce the problem to:

$$-d_k(c)\psi\omega^2 + d_k(\mu_{\sigma_k})(1-\psi)(\omega + \delta)^2 \geq -d_k(c)\psi(\omega + \delta)^2 + d_k(\mu_{\sigma_k})(1-\psi)\omega^2.$$

This is clearly true if $\psi \in (0, 1)$, however, for at least one $c \in \mathcal{S}$ we can impose a strict inequality since both $d_k(c) = 0$ and $d_k(\mu_{\sigma_k}) = 0$ cannot occur simultaneously for all c not equal to μ_{σ_k} . Thus:

$$\begin{aligned} & \Pr_{\text{sp}}(\pi_{\sigma_k} = \mu_{\sigma_k} \mid \pi_{\sigma_1}, \dots, \pi_{\sigma_{k-1}}, \boldsymbol{\mu}, \omega + \delta, \boldsymbol{\sigma}, \psi, p_b) \\ & > \Pr_{\text{sp}}(\pi_{\sigma_k} = \mu_{\sigma_k} \mid \pi_{\sigma_1}, \dots, \pi_{\sigma_{k-1}}, \boldsymbol{\mu}, \omega, \boldsymbol{\sigma}, \psi, p_b) \end{aligned}$$

for all $k = 2, \dots, n$. Since the inequality is true for an arbitrary $\boldsymbol{\sigma}$ and strict for at least one, it also strict when $\boldsymbol{\sigma}$ is integrated out of the model, therefore $\Pr(\boldsymbol{\pi}_1 = \boldsymbol{\mu}) < \Pr(\boldsymbol{\pi}_2 = \boldsymbol{\mu})$. \square

B.3 Proof of Theorem 3

Theorem 3: Consider two partition distributions: i) $p_{\boldsymbol{\mu}}$, a point mass at the anchor partition $\boldsymbol{\mu}$, and ii) $SP(\boldsymbol{\mu}, \boldsymbol{\omega}, \psi, p_b)$ such that $\boldsymbol{\omega} = \omega \times (1, \dots, 1)$ with $0 \leq \omega < \infty$, $\psi \in (0, 1)$, and $0 < p_b(\boldsymbol{\mu}) < 1$. If $\boldsymbol{\mu} \sim p_{\boldsymbol{\mu}}$ and $\boldsymbol{\pi} \sim SP(\boldsymbol{\mu}, \boldsymbol{\omega}, \psi, p_b)$ then:

- a) $D_{KL}(\boldsymbol{\mu}, \boldsymbol{\pi})$ is strictly decreasing as ω increases.
- b) $D_{TV}(\boldsymbol{\mu}, \boldsymbol{\pi})$ is strictly decreasing as ω increases.
- c) $E_{\boldsymbol{\mu}, \boldsymbol{\pi}} [RI(\boldsymbol{\mu}, \boldsymbol{\pi})] \rightarrow 1$ as $\omega \rightarrow \infty$.

Proof:

For the Kullback-Leibler divergence:

Let Π be the space of all partitions (of n items) and $0 \leq \omega < \omega + \delta \leq \infty$. Then the Kullback-Leibler divergence between $\boldsymbol{\mu} \sim p_{\boldsymbol{\mu}}$ and $\boldsymbol{\pi}_1 \sim SP(\boldsymbol{\mu}, \boldsymbol{\omega}, \psi, p_b)$ is:

$$\begin{aligned} D_{KL}(\boldsymbol{\mu}, \boldsymbol{\pi}_1) &= \sum_{\boldsymbol{\pi} \in \Pi} p_{\boldsymbol{\mu}}(\boldsymbol{\pi}) \log \left(\frac{p_{\boldsymbol{\mu}}(\boldsymbol{\pi})}{p_{\text{sp}}(\boldsymbol{\pi} \mid \boldsymbol{\mu}, \boldsymbol{\omega}, \psi, p_b)} \right) \\ &= 1 \cdot \log \left(\frac{1}{p_{\text{sp}}(\boldsymbol{\mu} \mid \boldsymbol{\mu}, \boldsymbol{\omega}, \psi, p_b)} \right) \\ &= -\log(p_{\text{sp}}(\boldsymbol{\mu} \mid \boldsymbol{\mu}, \boldsymbol{\omega}, \psi, p_b)) \end{aligned}$$

By Theorem 2 we know $p_{\text{sp}}(\boldsymbol{\mu} \mid \boldsymbol{\mu}, \boldsymbol{\omega}, \psi, p_b) < p_{\text{sp}}(\boldsymbol{\mu} \mid \boldsymbol{\mu}, \boldsymbol{\omega} + \delta, \psi, p_b)$. Transforming this equation we have $-\log(p_{\text{sp}}(\boldsymbol{\mu} \mid \boldsymbol{\mu}, \boldsymbol{\omega}, \psi, p_b)) > -\log(p_{\text{sp}}(\boldsymbol{\mu} \mid \boldsymbol{\mu}, \boldsymbol{\omega} + \delta, \psi, p_b))$. Thus if $\boldsymbol{\pi}_2 \sim SP(\boldsymbol{\mu}, \boldsymbol{\omega} + \delta, \psi, p_b)$, then $D_{KL}(\boldsymbol{\mu}, \boldsymbol{\pi}_2) < D_{KL}(\boldsymbol{\mu}, \boldsymbol{\pi}_1)$. \square

For the total variance distance:

We define the total variation distance between $\boldsymbol{\mu} \sim p_{\boldsymbol{\mu}}$ and $\boldsymbol{\pi}_1 \sim SP(\boldsymbol{\mu}, \boldsymbol{\omega}, \psi, p_b)$ to be:

$$D_{TV}(\boldsymbol{\mu}, \boldsymbol{\pi}_1) = \frac{1}{2} \sum_{\boldsymbol{\pi} \in \Pi} \left| p_{\boldsymbol{\mu}}(\boldsymbol{\pi}) - p_{\text{sp}}(\boldsymbol{\pi} \mid \boldsymbol{\mu}, \boldsymbol{\omega}, \psi, p_b) \right|.$$

This reduces to $1 - p_{\text{sp}}(\boldsymbol{\mu} \mid \boldsymbol{\mu}, \boldsymbol{\omega}, \psi, p_b)$, since $p_{\boldsymbol{\mu}}(\boldsymbol{\pi})$ is always zero except when $\boldsymbol{\pi} = \boldsymbol{\mu}$. By Theorem 2, $p_{\text{sp}}(\boldsymbol{\mu} \mid \boldsymbol{\mu}, \boldsymbol{\omega}, \psi, p_b) < p_{\text{sp}}(\boldsymbol{\mu} \mid \boldsymbol{\mu}, \boldsymbol{\omega} + \delta, \psi, p_b)$. Thus if $\boldsymbol{\pi}_2 \sim SP(\boldsymbol{\mu}, \boldsymbol{\omega} + \delta, \psi, p_b)$, then $D_{TV}(\boldsymbol{\mu}, \boldsymbol{\pi}_2) < D_{TV}(\boldsymbol{\mu}, \boldsymbol{\pi}_1)$. \square

For the expected Rand index converging to 1:

From Theorem 2 we know $P(\boldsymbol{\pi} = \boldsymbol{\mu}) = 1$ as $\omega \rightarrow \infty$. If $\boldsymbol{\pi} = \boldsymbol{\mu}$ with probability 1 then it is equivalent to show that the Rand index is equal to 1 with probability 1 or $P(RI(\boldsymbol{\mu}, \boldsymbol{\pi}) = 1) = 1$. Clearly $P(RI(\boldsymbol{\mu}, \boldsymbol{\pi}) = 1) = P(RI(\boldsymbol{\mu}, \boldsymbol{\pi}) \geq 1)$, then by the Markov inequality $P(RI(\boldsymbol{\mu}, \boldsymbol{\pi}) \geq 1) \leq E_{\boldsymbol{\mu}, \boldsymbol{\pi}}[RI(\boldsymbol{\mu}, \boldsymbol{\pi})]$. Thus in the limit as $\omega \rightarrow \infty$, $E_{\boldsymbol{\mu}, \boldsymbol{\pi}}[RI(\boldsymbol{\mu}, \boldsymbol{\pi})] = 1$. \square

B.4 Proof of Theorem 4

Theorem 4: *If $\boldsymbol{\pi}_1 \sim SP(\boldsymbol{\mu}, \boldsymbol{\omega}, \boldsymbol{\sigma}, \psi, p_b)$ and $\boldsymbol{\pi}_2 \sim SP(\boldsymbol{\mu}^*, \boldsymbol{\omega}, \boldsymbol{\sigma}, \psi, p_b)$, where $\boldsymbol{\mu}$ and $\boldsymbol{\mu}^*$ are anchor partitions such that for every i and j where $\omega_i > 0$ and $\omega_j > 0$, $\mu_i = \mu_j$ if and only if $\mu_i^* = \mu_j^*$, then $\boldsymbol{\pi}_1$ and $\boldsymbol{\pi}_2$ are equal in distribution.*

Proof:

To prove this theorem consider an arbitrary fixed partition $\boldsymbol{\rho}$. We show that under the conditions of the theorem $\Pr(\boldsymbol{\pi}_1 = \boldsymbol{\rho}) = \Pr(\boldsymbol{\pi}_2 = \boldsymbol{\rho})$, thus implying $\boldsymbol{\pi}_1$ is equal in distribution to $\boldsymbol{\pi}_2$.

Without loss of generality assume the items will be allocated using the natural permutation. From the CAPF in (2), with the permutation parameter removed, it is evident that both $\boldsymbol{\mu}$ and $\boldsymbol{\omega}$ only influence the exponential term. That exponential term is:

$$\exp\left(\frac{\omega_i}{i-1} \sum_{j=1}^{i-1} \omega_j \mathbb{I}\{\pi_j = c\} (\mathbb{I}\{\mu_j = \mu_i\} - \psi)\right).$$

For each $i \in \{2, \dots, n\}$ it is clear that:

$$\begin{aligned} & \exp\left(\frac{\omega_i}{i-1} \sum_{j=1}^{i-1} \omega_j \mathbb{I}\{\pi_j = c\} (\mathbb{I}\{\mu_j = \mu_i\} - \psi)\right) \\ &= \exp\left(\frac{\omega_i}{i-1} \sum_{j=1}^{i-1} \omega_j \mathbb{I}\{\pi_j = c\} (\mathbb{I}\{\mu_j^* = \mu_i^*\} - \psi)\right) \end{aligned}$$

since any time $\mu_j = \mu_i$ does not imply that $\mu_j^* = \mu_i^*$ (or vice versa) we have that either $\omega_i = 0$ or $\omega_j = 0$. Thus the CAPFs of $\boldsymbol{\pi}_1$ and $\boldsymbol{\pi}_2$ produce the same probabilities for an arbitrary partition. Additionally, the above equalities are not dependent on the allocation order of the items, and they also hold for any $\boldsymbol{\sigma}$. Therefore the pmfs for $\boldsymbol{\pi}_1$ and $\boldsymbol{\pi}_2$ produce the same probabilities for an arbitrary permutation and are equal in distribution. \square

B.5 Proof of Theorem 5

Theorem 5 Consider any baseline distribution p_b , anchor partition $\boldsymbol{\mu}$ and fixed partition $\boldsymbol{\rho}$, such that $p_b(\boldsymbol{\mu}) > 0$ and $p_b(\boldsymbol{\rho}) > 0$. For any $\boldsymbol{\omega} = \omega \times (s_1, \dots, s_n)$ with s_i either 0 or 1, and $\psi \in (0, 1)$, define \mathcal{Q} to be the set of index pairs (i, j) such that $\omega_i > 0$, $\omega_j > 0$, and $\mu_i = \mu_j$. If $\rho_i = \rho_j$ for all index pairs in \mathcal{Q} , then $\boldsymbol{\rho}$ is a limiting partition of $\boldsymbol{\pi} \sim SP(\boldsymbol{\mu}, \boldsymbol{\omega}, \psi, p_b)$.

Proof: The crux of the proof is to show under the theorem's conditions and with $\boldsymbol{\pi} \sim SP(\boldsymbol{\mu}, \boldsymbol{\omega}, \boldsymbol{\sigma}, \psi, p_b)$ then:

$$\lim_{\omega \rightarrow \infty} \Pr(\boldsymbol{\pi} = \boldsymbol{\rho}) > 0.$$

First consider a restricted permutation $\boldsymbol{\sigma}^*$, such that all items with $s_i = 1$ are allocated first, and the items with $s_i = 0$ are allocated afterwards. For the items with $s_i = 1$, any time $\mu_{\sigma_i} = \mu_{\sigma_j}$ we have that $\rho_{\sigma_i} = \rho_{\sigma_j}$. Therefore $\boldsymbol{\rho}$ has a probability of 1 up to that point

in the allocation (see Theorem 1). Now as the final items with $s_i = 0$ are allocated each of their CAPFs must also be nonzero since $p_b(\boldsymbol{\rho}) > 0$. Thus for any permutation $\boldsymbol{\sigma}^*$ in that restricted class

$$\lim_{\omega \rightarrow \infty} \Pr(\boldsymbol{\pi} = \boldsymbol{\rho}) > 0.$$

Now consider an arbitrary permutation $\boldsymbol{\sigma}$. If the allocation order of an item with $s_i = 0$ is moved before an item with $s_i = 1$, we have the following:

1. The exponential term in the SP's CAPF is simply 1 and the item is allocated using the probabilities of p_b , which still must be positive.
2. Additionally, for the item with $s_i = 1$, the sums in its exponential term of the SP's CAPF, (2), are unchanged whether or not an item with $s_i = 0$ is allocated before it or not. These sums produced a positive exponential term in CAPF for the case with the restricted $\boldsymbol{\sigma}^*$, thus they must also produce a positive CAPF value when considering an arbitrary $\boldsymbol{\sigma}$ (with the condition that $p_b(\boldsymbol{\rho}) > 0$).

These two arguments can be iterated any number of times to produce any $\boldsymbol{\sigma}$ by permuting the order of $\boldsymbol{\sigma}^*$ one item at a time. Therefore we have that $\boldsymbol{\rho}$ is a limiting partition of $SP(\boldsymbol{\mu}, \boldsymbol{\omega}, \boldsymbol{\psi}, p_b)$. □

B.6 Proof of Theorem 6

Theorem 6 *Let $\boldsymbol{\pi} \sim SP(\boldsymbol{\mu}, \boldsymbol{\omega}, \boldsymbol{\sigma}, \boldsymbol{\psi}, p_b)$, with $p_b(\boldsymbol{\pi}) > 0$ for all possible $\boldsymbol{\pi}$ and $\boldsymbol{\omega} = \omega \times (s_1, \dots, s_n)$, where s_i is either 0 or 1 and $\boldsymbol{\psi} \in (0, 1)$. Let $a = n - \sum_{i=1}^n s_i$ be the number of items with shrinkage equal to zero. Let b be the number of clusters in $\boldsymbol{\mu}$ having at least one item with $s = 1$. As $\omega \rightarrow \infty$, the number of limiting partitions in the SP distribution is $B(a, b)$.*

Proof: There are n items being partitioned, with a items that have an idiosyncratic shrinkage parameter of zero. There are also b clusters in $\boldsymbol{\mu}$ that have least 1 item such that

$\omega_i > 0$.

Without loss of generality, let the $n - a$ items with $\omega_i > 0$ be allocated first. By Theorem 1, with probability 1, they must be allocated to agree with $\boldsymbol{\mu}$ (since $\omega \rightarrow \infty$). Thus there is only one possible partition for those $n - a$ items. Now if the other a items are allocated, there are exactly b existing clusters and a items to be allocated, thus there are exactly $B(a, b)$ possible partitions (see Appendix A). The item allocation order can change the probability of a possible partition, but in this case it cannot change the number of possibilities that have probability greater than zero. □

Appendix C Details of the MCMC Algorithms

This appendix provides details of the MCMC algorithms used in Section 6. Software implementing our SP distribution is available as an R package (<https://github.com/dbdahl/gourd-package>). Table 2 reiterates notation. Section C.1 introduces the most intricate aspect of the MCMC involving our SP distribution, which is updating the random partition based on a modification of Neal’s Algorithm 8 (Neal, 2000). Then, Sections C.2 - C.4 explain the sampling details use for the independent model in Section 6.1, the hierarchical model in Section 6.2, and the temporal model in Section 6.3, respectively.

Symbol	Description
n	Number of states in the US (including the District of Columbia), i.e., $n = 51$.
T	Total number of years under consideration, i.e., $T = 27$.
\mathbf{I}	An identity matrix.
n_{it}	Number of observations in the i^{th} state and t^{th} year.
n_{ct}	Sum of the n_{it} of each state for the t^{th} year and in cluster c .
\mathbf{y}_t	Log hourly earnings for individuals in the t^{th} year, length $\sum_{i=1}^n n_{it}$.
\mathbf{y}_{ct}	Log hourly earnings for individuals in the c^{th} cluster and t^{th} year, length n_{ct} .
\mathbf{y}_{it}	Log hourly earnings for individuals in the i^{th} state and t^{th} year, length n_{it} .
\mathbf{Z}_t	Demographic covariates for individuals in the t^{th} year, dimension $\sum_{i=1}^n n_{it} \times 9$.
\mathbf{Z}_{ct}	Demographic covariates for the c^{th} cluster and t^{th} year, dimension $n_{ct} \times 9$.
\mathbf{Z}_{it}	Demographic covariates for the i^{th} state and t^{th} year, dimension $n_{it} \times 9$.
$\boldsymbol{\gamma}_t$	Common regression coefficients for the t^{th} year associated with \mathbf{Z}_t , length 9.
\mathbf{X}_{ct}	Intercept and education dummy variables for the c^{th} cluster and t^{th} year, dimension $n_{ct} \times 4$.
\mathbf{X}_{it}	Intercept and education dummy variables for the i^{th} state and t^{th} year, dimension $n_{it} \times 4$.
$\boldsymbol{\beta}_{ct}^*$	Coefficients for intercept and education dummy variables associated with \mathbf{X}_{ct} , length 4.
$\boldsymbol{\beta}_{it}$	Coefficients for intercept and education dummy variables associated with \mathbf{X}_{it} , length 4.
τ_t	Model precision for the t^{th} year.
p_{sp}	Probability mass function (pmf) of the SP distribution, given in (3).
$\boldsymbol{\pi}_t$	Partition cluster labels in canonical form for the t^{th} year, length n .
q_t	Number of clusters in a given $\boldsymbol{\pi}_t$.
$\boldsymbol{\mu}$	Cluster labels in canonical form, defining the anchor for all years, length n .
$\boldsymbol{\mu}_t$	Cluster labels in canonical form, defining anchor for the t^{th} year, length n .
$\boldsymbol{\omega}$	The shrinkage parameter in the SP distribution, length n .
$\boldsymbol{\sigma}_t$	Permutation of $1, 2, \dots, n$ used to define the order of item allocation for $\boldsymbol{\pi}_t$, length n .
$\boldsymbol{\rho}_r$	A fixed partition defined by the US Census Regions as shown in Figure 3, length n .
$\boldsymbol{\rho}_s$	A fixed partition defined by a random shuffle of $\boldsymbol{\rho}_r$, length n .
ψ	Grit parameter in the SP distribution, typically in $(0, 1)$.
p_b	Baseline partition distribution of the SP distribution.

Table 2: Notational summary. Lower case bolded items are vectors, and capitalized bolded items are matrices.

C.1 Updating the Partition

Our MCMC update of a partition with an SP prior follows a modification of Neal’s Algorithm 8, where each step updates a cluster label of a given item conditional on the allocation of all other items. At each step, we assume for notational convenience that the partition $\boldsymbol{\pi}_t$ is represented in cluster label notation using a canonical form, i.e., each element of the vector has a value $c = 1, \dots, q_t$ and, according to the permutation, 1 must appear before 2, 2 before 3, etc. For a fixed year t (where $t = 1, \dots, 27$) and i (where $i = 1, \dots, n$), update the cluster label of the σ_{ti}^{th} item using the following steps:

1. Define q_t to be the current number of clusters in $\boldsymbol{\pi}_t$, let $\boldsymbol{\pi}_t^*$ to be identical to $\boldsymbol{\pi}_t$ with the exception that $\pi_{t\sigma_{ii}}^* = c$, and let $\mathbf{y}_{it} \mid \boldsymbol{\beta}_{ct}^*, \boldsymbol{\gamma}_t, \tau_t \sim \text{N}(\mathbf{X}_{it}\boldsymbol{\beta}_{ct}^* + \mathbf{Z}_{it}\boldsymbol{\gamma}_t, \tau_t\mathbf{I})$, i.e., $p(\mathbf{y}_{it} \mid \boldsymbol{\beta}_{ct}^*, \boldsymbol{\gamma}_t, \tau_t)$ is a multivariate normal density with precision $\tau_t\mathbf{I}$. Then for $c = 1, \dots, q_t$, calculate

$$p(\mathbf{y}_{it} \mid \boldsymbol{\beta}_{ct}^*, \boldsymbol{\gamma}_t, \tau_t) \times p_{\text{sp}}(\boldsymbol{\pi}_t^* \mid \boldsymbol{\mu}, \boldsymbol{\omega}, \boldsymbol{\sigma}_t, \psi, p_b). \quad (16)$$

2. If the σ_{ti}^{th} item is not currently in a singleton cluster, draw a value of $\boldsymbol{\beta}_{ct}^*$ from a $\text{N}(\boldsymbol{\mu}_\beta, \tau_\beta\mathbf{I})$ and once again calculate (16), where $c = q_t + 1$. That is, we only propose one possible new cluster (i.e., $m = 1$ in the notation of Neal’s Algorithm 8). It appears to be straightforward to allow for the $m > 1$ case, if desired.
3. With probabilities proportional to the quantities calculated in the previous two steps, randomly select which cluster the σ_{ti}^{th} item is reassigned. We note that there are computational efficiencies in (16) and subsequent equations since the CAPF terms for items $1, \dots, i - 1$ are the same for all possible clusters c and would therefore cancel in the quantities calculated in this step.

One iteration of the algorithm involves repeating the previous steps for each of the n times.

C.2 Independent Models

We now describe the details of the MCMC scheme for the SP models of Section 6.1. Although there are actually two SP models, they only differ in their fixed value of ω . Each step of the MCMC is the same, thus we will refer to it as a single model.

The details of how the parameters are updated, and initialized, are given below. The numbered ordering below is arbitrary, these could be rearranged without any impact to the scheme’s validity.

1. π_t : The prior for each $\pi_t \mid \mu_t, \omega, \sigma_t, \psi, p_b$ is an independent $\text{SP}(\mu_t, \omega, \sigma_t, \psi, p_b)$. This is a one-item-at-a-time Gibbs update. For each year t , update the partition according to the steps in Section C.1. The value of π_t is initialized at the fixed value of ρ_r and p_b is the $\text{CRP}(1)$; the other parameters are described below.
2. μ_t : In this model, the anchor for each year is fixed at ρ_r , so no MCMC updates are needed.
3. σ_t : The prior for each σ_t is a discrete uniform over the space of permutations (*iid* for all t). This is a Metropolis update within Gibbs; for each year t , 10 positions in the current permutation vector σ_t^c were randomly selected. Then the values of those 10 positions were randomly shuffled, with the 41 other positions remaining fixed. This modified permutation vector is the proposal σ_t^* . Since the proposal distribution is symmetric, and the likelihood does not depend on the permutation, this proposal is accepted with probability

$$\min \left(1, \frac{p_{\text{sp}}(\pi_t \mid \mu, \omega, \sigma_t^*, \psi, p_b)}{p_{\text{sp}}(\pi_t \mid \mu, \omega, \sigma_t^c, \psi, p_b)} \right).$$

This Metropolis update procedure is repeated 9 more times to improve mixing. The specific choice of shuffling 10 positions and 10 Metropolis updates are tuning details, which can be increased or decreased as appropriate. σ_t is initialized at the natural permutation, $(1, 2, \dots, n)$.

4. β_{ct}^* : The prior for each state and year is $\beta_{it} \sim N(\boldsymbol{\mu}_\beta, \tau_\beta \mathbf{I})$, *iid* for all i and t . In this model, we set $\boldsymbol{\mu}_\beta = (1.46, 0.15, 0.24, 0.41)'$ and $\tau_\beta = 100$. This step is a Gibbs update. For each combination of c and t , draw an update as follows:

$$\beta_{ct}^* \mid \cdot \sim N \left(\left[\tau_t \mathbf{X}'_{ct} \mathbf{X}_{ct} + \tau_\beta \mathbf{I} \right]^{-1} \left[\tau_t \mathbf{X}'_{ct} (\mathbf{y}_{ct} - \mathbf{Z}_{ct} \boldsymbol{\gamma}_t) + \tau_\beta (\boldsymbol{\mu}_\beta - \mathbf{Z}_{ct} \boldsymbol{\gamma}_t) \right], \tau_t \mathbf{X}'_{ct} \mathbf{X}_{ct} + \tau_\beta \mathbf{I} \right).$$

We note here that the second argument in the normal distribution is a precision (not a variance or standard deviation). Additionally, the “ \cdot ” in the conditioning symbol is used to denote all other parameters, without enumerating them. Since $\boldsymbol{\pi}_t$ is initialized at the census regions (i.e., it has four clusters), the four corresponding β_{ct}^* 's for each year are initialized by drawing from their independent $N(\boldsymbol{\mu}_\beta, \tau_\beta \mathbf{I})$ priors.

5. $\boldsymbol{\gamma}_t$: The prior for each year is $\boldsymbol{\gamma}_t \sim N(\mathbf{0}, \tau_\gamma \mathbf{I})$, *iid* for all t . In this model we set $\tau_\gamma = 1$. This MCMC step is a Gibbs update. For each year t , draw an update as follows:

$$\boldsymbol{\gamma}_t \mid \cdot \sim N \left(\left[\tau_t \mathbf{Z}'_t \mathbf{Z}_t + \tau_\gamma \mathbf{I} \right]^{-1} \left[\tau_t \mathbf{Z}'_t \left(\mathbf{y}_t - \begin{bmatrix} \mathbf{X}_{1t} \boldsymbol{\beta}_{1t} \\ \vdots \\ \mathbf{X}_{nt} \boldsymbol{\beta}_{nt} \end{bmatrix} \right) \right], \tau_t \mathbf{Z}'_t \mathbf{Z}_t + \tau_\gamma \mathbf{I} \right).$$

The value of $\boldsymbol{\gamma}_t$ is initialized by a random draw from its prior $N(\mathbf{0}, \tau_\gamma \mathbf{I})$, independently for each year.

6. τ_t : The prior for each year is $\tau_t \sim \text{Gamma}(\alpha_\tau, \beta_\tau)$, *iid* for all t . We set $\alpha_\tau = 1/0.361^2$, and $\beta_\tau = 1$. This step is a Gibbs update. For each year t , draw an update as follows:

$$\tau_t \mid \cdot \sim \text{Gamma} \left(\alpha_\tau + \frac{1}{2} \sum_{i=1}^n n_{it}, \beta_\tau + \frac{1}{2} \sum_{i=1}^n (\mathbf{y}_{it} - \mathbf{X}_{it} \boldsymbol{\beta}_{it} - \mathbf{Z}_{it} \boldsymbol{\gamma}_t)' (\mathbf{y}_{it} - \mathbf{X}_{it} \boldsymbol{\beta}_{it} - \mathbf{Z}_{it} \boldsymbol{\gamma}_t) \right).$$

We use the rate parameterization of the gamma distribution. The value of τ_t is initialized by a random draw from its prior, independently for each year.

7. $\boldsymbol{\omega}$: The difference in the two independent models is solely the choice of $\boldsymbol{\omega}$. In the independent model with common shrinkage $\boldsymbol{\omega} = (5, \dots, 5)$, i.e., all states have a shrinkage

value of 5. For the independent model with idiosyncratic shrinkage, each state had a shrinkage value set to 5 except for Maryland, Delaware, District of Columbia, Montana, North Dakota, and South Dakota, whose shrinkage values were set to 1. Since these vectors are fixed, no MCMC update is needed.

8. ψ : In the independent model, the grit parameter is fixed at 0.02. Therefore, no updates are needed.

This model allows for each year to be run in parallel.

C.3 Hierarchical Model

This section provides the MCMC details for the hierarchical model in Section 6.2. This model is similar to the independent model described in the previous section. The primary difference is that each state now has a common anchor partition, which itself has a prior distribution. The following list describes how the parameters are updated and initialized.

1. π_t : The prior for each $\pi_t \mid \mu, \omega, \sigma_t, \psi, p_b$ is an independent $\text{SP}(\mu, \omega, \sigma_t, \psi, p_b)$. For each year, update the partition according to the steps in Section C.1. The value of π_t is initialized by randomly (and uniformly) drawing a value from $\{1, 2, 3, 4, 5\}$ for each state. The π_t for each year t , is given the same initial value. p_b is the $\text{CRP}(1)$, and the other parameters are described below.
2. μ : In this model, the anchor is common across all years, which permits the borrowing of strength between all π_t . The prior is $\mu \sim \text{SP}(\rho_r, \omega_0, \sigma_0, \psi_0, p_b)$, where p_b is the $\text{CRP}(1)$. In the following sub-steps we show how μ and its associated hyperparameters are updated.
 - a) To update μ , we use a one-at-a-time Gibbs update based on Algorithm 8 in Neal (2000). For all $i = 1, \dots, n$ repeat the following steps:

- i) Let q_μ be equal to the number of clusters in the current value of μ , and let μ^* be identical to μ , except that $\mu_{\sigma_{0i}}^* = c$. Then, for $c = 1, \dots, q_\mu$, calculate the following quantity:

$$\left(\prod_{t=1}^T p_{\text{sp}}(\pi_t \mid \mu^*, \omega, \sigma_t, \psi, p_b) \right) \times p_{\text{sp}}(\mu^* \mid \rho_r, \omega_0, \sigma_0, \psi_0, p_b). \quad (17)$$

- ii) If the σ_{0i}^{th} item of μ is not currently in a singleton cluster, set μ^* to be equal to μ except that $\mu_{\sigma_{0i}}^* = q_\mu + 1$. Then calculate (17) again. If the σ_{0i}^{th} item of μ is in a singleton cluster, omit this step.
- iii) With probabilities proportional to the quantities calculated in the previous two steps, randomly allocate the σ_{0i}^{th} item to a cluster.
- b) σ_0 : This is the same as described in Section C.2, except that only 5 positions in the proposed permutation vector are shuffled.
- c) ω_0 : ω_0 is defined as $\omega_0 \times (a_{\sigma_{01}}, a_{\sigma_{02}}, \dots, a_{\sigma_{0n}})$, where $a_{\sigma_{0i}}$ is equal to 1, except for Maryland, Delaware, District of Columbia, Montana, North Dakota, and South Dakota whose $a_{\sigma_{0i}}$ values are set to 0.2. The prior for ω_0 is a Gamma(5, 1) and ω_0 is updated via slice sampling with step size of $\sqrt{5}$. It is initialized with a random draw from its prior.
- d) ψ_0 : The prior for ψ_0 is a uniform on the unit interval. This parameter is updated using the slice sampler with a step size of $1/\sqrt{12}$. The initial value of ψ_0 is randomly drawn from its prior.
3. σ_t : This is the same as described in Section C.2, except that only 5 positions in the proposed permutation vector are shuffled, to improve acceptance rates.
4. β_{ct}^* : This is the same as described in Section C.2.
5. γ_t : This is the same as described in Section C.2.
6. τ_t : This is the same as described in Section C.2.

7. ω : Let $\omega = \omega \times (1, \dots, 1)$ and assume $\omega \sim \text{Gamma}(5, 1)$. Update using a slice sampler with a step size of $\sqrt{5}$. The value of ω is initialized by taking a draw from its prior.
8. ψ : The prior for ψ is a uniform on the unit interval. This parameter is also updated using the slice sampler, with a step size of $1/\sqrt{12}$. The initial value of ψ is randomly drawn from its prior.

C.4 Temporally-Dependent Model

The temporally-dependent model, as implemented in Section 6.3, has many common aspects of the previous models. However, in this model, we do not define a μ (except at year $t = 1$) since we use the previous year's partition π_{t-1} as the anchor for the current year. In this model all baseline distributions p_b are the CRP(1).

1. π_1 : The prior for $\pi_1 \mid \rho_r, \omega_1, \sigma_1, \psi_1, p_b$ is an independent $\text{SP}(\rho_r, \omega_1, \sigma_1, \psi_1, p_b)$.
 - a) To update π_1 , we again use a one-at-a-time Gibbs update based on Neal's Algorithm 8. For all $i = 1, \dots, n$, repeat the following steps:
 - i) Let q_{π_1} be the number of clusters in current version of π_1 , and define π_1^* to be identical to π_1 , except that $\pi_{1\sigma_{1i}}^* = c$. Then, for $c = 1, \dots, q_{\pi_1}$, compute the following quantity:
$$p(\mathbf{y}_{i1} \mid \beta_{c1}^*, \gamma_1, \tau_1) \times p_{\text{sp}}(\pi_1^* \mid \rho_r, \omega_1, \sigma_1, \psi_1, p_b), \times p_{\text{sp}}(\pi_2 \mid \pi_1^*, \omega, \sigma_2, \psi, p_b). \quad (18)$$
 - ii) If the σ_{1i}^{th} item of π_1 is not currently in a singleton cluster, set π_1^* to be equal to π_1 except that $\pi_{1\sigma_{1i}}^* = q_{\pi_1} + 1$. Then calculate (18) again. If the σ_{1i}^{th} item of π_1 is in a singleton cluster, omit this step.
 - iii) With probabilities proportional to the quantities calculated in the previous two steps, randomly select the cluster to which the σ_{1i}^{th} item of π_1 is reassigned.

- b) σ_1 : This is the same as described in Section C.2, except that only 5 positions in the proposed permutation vector are shuffled.
- c) ω_1 : ω_1 is defined as $\omega_1 \times (a_{\sigma_{11}}, a_{\sigma_{12}}, \dots, a_{\sigma_{1n}})$, where $a_{\sigma_{1i}}$ is equal to 1, except for Maryland, Delaware, District of Columbia, Montana, North Dakota, and South Dakota whose $a_{\sigma_{1i}}$ values are 0.2. The prior for ω_1 is a Gamma(5, 1). ω_1 is updated via slice sampling, with step size of $\sqrt{5}$, and it is initialized with a random draw from its prior.
- d) ψ_1 : The prior for ψ_1 is a uniform on the unit interval. This parameter is updated using the slice sampler with a step size of $1/\sqrt{12}$. The initial value of ψ_1 is randomly drawn from its prior.
2. π_t for $t = 2, \dots, T$: The prior for $\pi_t \mid \pi_{t-1}, \omega, \sigma_t, \psi, p_b$ is an independent SP($\pi_{t-1}, \omega, \sigma_t, \psi, p_b$). This is a one-at-a-time Gibbs update based on Neal’s Algorithm 8. The value of each π_t (including π_1), is initialized the same as in Section C.3. For each year $t = 2, \dots, T$ and for all $i = 1, \dots, n$, repeat the following steps:
- a) Let q_{π_t} to equal to the number of clusters in the current value of π_t . Additionally, set π_t^* to be identical to π_t , with the exception that $\pi_{t\sigma_{ti}}^* = c$. Then for $c = 1, \dots, q_{\pi_t}$, compute the following quantity:
- $$p(\mathbf{y}_{it} \mid \beta_{ct}^*, \gamma_t, \tau_t) \times p_{\text{sp}}(\pi_t^* \mid \pi_{t-1}, \omega, \sigma_t, \psi, p_b) \times p_{\text{sp}}(\pi_{t+1} \mid \pi_t^*, \omega, \sigma_{t+1}, \psi, p_b). \quad (19)$$
- Note: When $t = T$ the last term should be omitted from (19).
- b) If the σ_{ti}^{th} item of π_t is not currently in a singleton cluster, set π_t^* to be equal to π_t , with the exception that $\pi_{t\sigma_{ti}}^* = q_{\pi_t} + 1$. Then calculate (19) again. If the σ_{ti}^{th} item of π_t is in a singleton cluster, omit this step.
- c) With probabilities proportional to the quantities calculated in the previous two steps, randomly select the cluster to which the σ_{ti}^{th} item of π_t is reassigned.

3. σ_t : This is the same as described in Section C.3, except the acceptance probability is now:

$$\min \left(1, \frac{p_{\text{sp}}(\boldsymbol{\pi}_t \mid \boldsymbol{\pi}_{t-1}, \boldsymbol{\omega}, \boldsymbol{\sigma}_t^*, \psi, p_b)}{p_{\text{sp}}(\boldsymbol{\pi}_t \mid \boldsymbol{\pi}_{t-1}, \boldsymbol{\omega}, \boldsymbol{\sigma}_t^c, \psi, p_b)} \right).$$

4. β_{ct}^* : This is the same as described in Section C.2.
5. γ_t : This is the same as described in Section C.2.
6. τ_t : This is the same as described in Section C.2.
7. ω : This is the same as described in Section C.3.
8. ψ : This is the same as described in Section C.3.

Appendix D US Census Regions

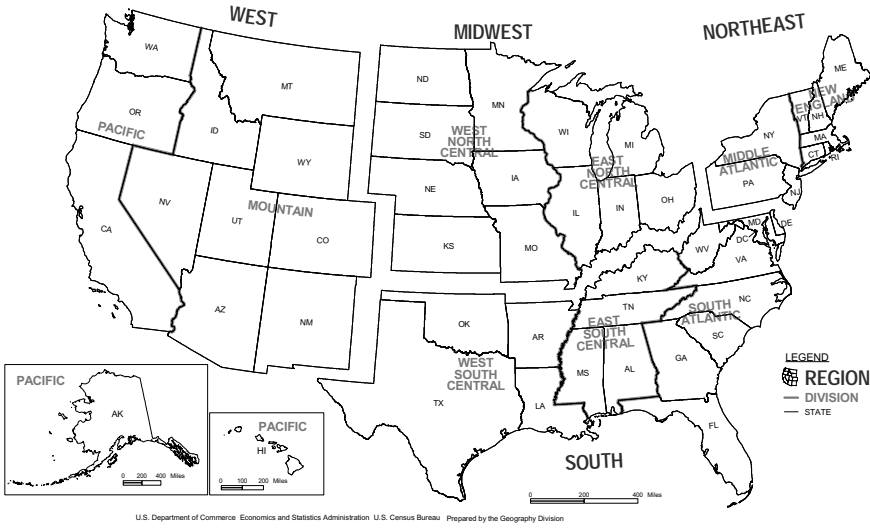
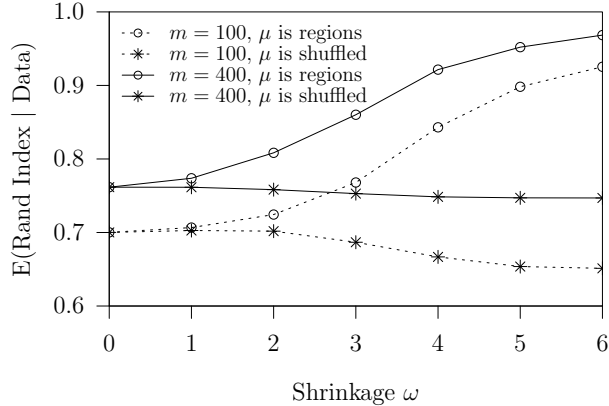


Figure 3: The four regions defined by U.S. Census Bureau are used as a prior anchor partition in the education regression example in Subsection 6.1 in which the regression coefficients for the 50 states and the District of Columbia are clustered.

Appendix E Cluster Estimation

To study cluster estimation, we use the same model as Section 6.1 and only consider one year (so we drop t in the notation). The values of the model parameters in the simulation were based on OLS estimates from the IPUMS data in Section 6, using a model without state-specific intercepts and slopes. For 50 of the simulated datasets, each of the $n = 51$ simulated states had exactly $m = 100$ observations. Another 50 datasets were simulated with $m = 400$ observations. Responses for each dataset were generated from the sampling model as follows. The regression coefficient vector γ for the non-education covariates was set at the OLS estimates and the covariate values were sampled from the actual data for each state. The regions partition ρ_r was used to generate data from four clusters and the education coefficients β_c^* for each cluster were deviations from the OLS estimates. The education covariate values were sampled from the actual data for each state. The error precision for the simulated data was obtained from the OLS estimate.

The posterior expected Rand index $E(\text{RI}(\boldsymbol{\pi}, \boldsymbol{\rho}_r) \mid \mathbf{y})$ is displayed on the left hand side of Figure 4. Specifically, we assume $\boldsymbol{\pi} \sim \text{SP}(\boldsymbol{\mu}, \boldsymbol{\omega}, \boldsymbol{\sigma}, \psi, \text{JLP}(1))$ with $\boldsymbol{\omega} = \omega \times (1, \dots, 1)$ for $\omega = 0, 1, \dots, 6$, $\boldsymbol{\sigma}$ having a discrete uniform distribution, and ψ having a Beta(2, 2) distribution (to match the prior elicitation in the next paragraph). We let $\boldsymbol{\mu}$ equal either the regions partition $\boldsymbol{\rho}_r$ or the partition $\boldsymbol{\rho}_s$ obtained by randomly shuffling the region labels. When $\boldsymbol{\mu} = \boldsymbol{\rho}_r$, i.e., the partition from which the data was generated, the posterior expected Rand index improves with increasing shrinkage ω . Conversely, when assuming $\boldsymbol{\mu} = \boldsymbol{\rho}_s$, this mistake leads to worsening posterior expected Rand index as the shrinkage ω increases. Also, note that the posterior expected Rand index improves with the sample size m increasing from 100 to 400. The upshot is that the SP distribution behaves as one would expect in a typical Bayesian model, improving estimation when prior assumptions are met, worsening estimation when prior assumptions are bad, and yielding to the data as the sample size increases.



		E(Rand Index Data) w/ Anchor μ Being...	
m	Distribution	Regions	Shuffled
100	SP w/ random ω and ψ	(0.91, 0.94)	(0.68, 0.70)
100	LSP w/ random ω	(0.86, 0.88)	(0.68, 0.69)
100	CPP-VI w/ fixed ω	(0.85, 0.87)	(0.62, 0.64)
100	CPP-B w/ fixed ω	(0.93, 0.94)	(0.72, 0.73)
400	SP w/ random ω and ψ	(0.96, 0.98)	(0.75, 0.76)
400	LSP w/ random ω	(0.93, 0.95)	(0.74, 0.75)
400	CPP-VI w/ fixed ω	(0.93, 0.94)	(0.74, 0.75)
400	CPP-B w/ fixed ω	(0.97, 0.98)	(0.77, 0.78)

Figure 4: Left: The posterior expected Rand index for the true partition ρ_r used to generate the data and models with the SP distribution, as a function of the shrinkage ω , the assumed anchor μ , and the sample size m . Right: The posterior expected Rand index for the true partition ρ_r for various prior distributions, all of which have been calibrated to have the same prior expected Rand index as the SP distribution. 95% confidence intervals are shown.

Before comparing the SP, LSP, and CPP distributions for partition estimation, we first need to consider the prior on the shrinkage parameter ω and grit parameter ψ and then how to make the LSP and CPP distributions put the same amount of prior information on the anchor partition. We use the prior elicitation method outlined in Section 4.3. Consider shrinkage values $\omega = \omega \times (1, \dots, 1)$ from ω on a grid ranging from 0 to 10 and grid of grit values ψ from 0 to 1. For each combination of ω and ψ values, sample many partitions from the SP distribution using uniformly-sampled permutations, a JLP(1) baseline distribution, and the anchor set to ρ_r and then compute Monte Carlo estimates of $E(\text{RI}(\pi, \rho_r))$ and $E(\text{Entropy}(\pi))$. The left and middle panels of Figure 5 show heatmap plots of the expected Rand index (left) and the expected entropy (middle). Notice that the shrinkage ω has a strong influence on the expected Rand index whereas the grit ψ substantially changes the expected cluster entropy. The plots also show joint density contours for $\omega \sim \text{Gamma}(4, 1)$ and $\psi \sim \text{Beta}(2, 2)$. We suggest this is a justifiable joint prior since the distribution has substantial density for a wide range of values for the Rand index and entropy, but one could

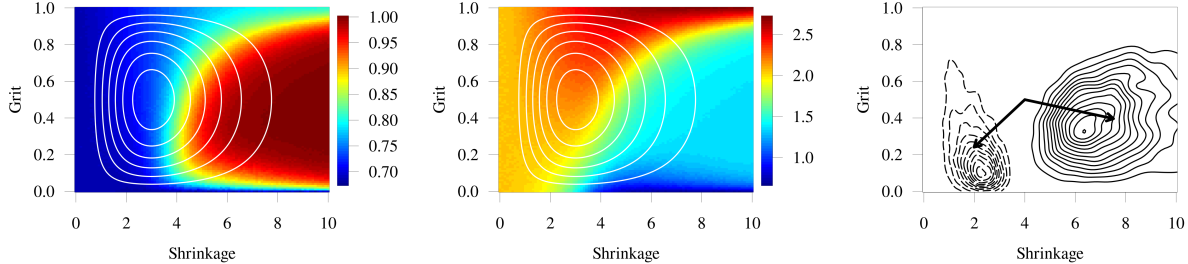


Figure 5: Left: Prior density of the joint prior on the shrinkage ω and the grit ψ in white contours, with the prior expected Rand index in color. Middle: Same as left plot, except the prior expected entropy is in color. Right: Posterior densities of the shrinkage ω and the grit ψ for misspecified anchor ρ_s (dashed) and the correctly specified anchor ρ_r (solid). The arrows indicate the movement of the prior mean to the posterior means.

modify the prior specification for ω and ψ if the contours in the heatmap plots do not align with prior expectations. The right plot of Figure 5 show contours of the joint posterior density of the shrinkage ω and the grit ψ for the first simulated dataset with $m = 400$ — the other 49 datasets look similar — for the model with $\mu = \rho_r$ (in solid curves) and $\mu = \rho_s$ (in dashed curves). The movement from the prior mean to the posterior means (indicated by the arrows) is also shown. It is reassuring that the posterior density moves toward higher shrinkage values when correctly assuming $\mu = \rho_r$ and toward smaller shrinkage values when mistakenly assuming $\mu = \rho_s$. The separation of the prior and posterior densities indicate substantial posterior learning on the shrinkage ω and grit ψ parameters.

Now we compare the SP, LSP, and CPP distributions for partition estimation. Recall that LSP reduces to JLP(1) when shrinkage $\omega = 0$, so we use JLP(1) as the baseline distribution for SP and CPP for the sake of comparison. We want to compare the models for a finite shrinkage using both a correctly specified anchor $\mu = \rho_r$ and a misspecified anchor $\mu = \rho_s$. Since the SP, LSP, and CPP have different formulations, each distribution must be calibrated such that it imbues the same degree of belief in the anchor μ . To this end, we computed the prior expected Rand index $E(\text{RI}(\pi, \mu))$ for the SP distribution with $\omega \sim \text{Gamma}(4, 1)$ and

$\psi \sim \text{Beta}(2, 2)$ under both anchors $\boldsymbol{\mu} = \boldsymbol{\rho}_r$ and $\boldsymbol{\mu} = \boldsymbol{\rho}_s$. We then found, for each anchor, a u such that the LSP with a $\text{Gamma}(u, 1)$ prior on its shrinkage parameter led to the same prior expected Rand index as the SP distribution for that anchor. We did likewise for the CPP with Binder loss and VI loss, except we found fixed shrinkage values since the CPP cannot accommodate priors on hyperparameters. With these calibrated priors, we fit the model for our 100 simulated datasets and the table on the right hand side of Figure 4 shows 95% confidence intervals on the Monte Carlo estimates of $E(\text{RI}(\boldsymbol{\pi}, \boldsymbol{\rho}_r) \mid \mathbf{y})$. Note that, for both $m = 100$ and $m = 400$, the SP distribution performs about as well as the CPP with Binder loss when the anchor is the truth (i.e., $\boldsymbol{\mu} = \boldsymbol{\rho}_r$) and better than LSP and CPP with VI loss. This is interesting because the CPP with Binder loss performed poorly in Section 6.1, yet performs well here. When the anchor is mistaken (i.e., $\boldsymbol{\mu} = \boldsymbol{\rho}_s$), most of the 95% confidence intervals overlap. We also found (but do not show) that the SP distribution with $\boldsymbol{\mu} = \boldsymbol{\rho}_r$ is the best in terms of $E(\text{VI}(\boldsymbol{\pi}, \boldsymbol{\rho}_r) \mid \mathbf{y})$ and has non-overlapping confidence intervals with the LSP and CPP with both Binder and VI losses. We conclude that the SP distribution is competitive in cluster estimation while also being amenable to posterior inference on hyperparameters (due to its tractable normalizing constant) and ready-made for dependent modeling (as demonstrated in Section 6).